RECORD No. 1966/86

011218

GRAVITY ANOMALY
OF A SLOPING CONTACT

by

J.C. DOOLEY

GRAVITY ANOMALY
OF A SLOPING CONTACT

by

J.C. DOOLEY

CONTENTS

ILLUSTRATIONS

SUMMARY

Gravity anomalies have been calculated in normalised co-ordinates for a two-dimensional, semi-infinite horizontal slab, or wedge, bounded on one side by a sloping surface. This is a schematic equivalent of geological features such as faults, monoclines, or the boundaries of igneous intrusions if extended in length and width.

Curves are presented in normalised co-ordinates and also in bilogarithmic co-ordinates for slopes of $5°$, $10°$, $15°$, $30°$, $45°$, $60°$, $75°$ and $90°$, and for ratios of depths of upper to lower boundary of the slab of 0, 0.1, 0.2, 0.32, 0.5, and 0.8. If it is assumed that only one slope and one density contrast are involved, it is shown that theoretically there should be a unique solution in terms of dip angle and depth ratio; however, the differences between the curves for depth ratios of 0.5 or greater are small, and in practice a unique solution could not be obtained for these cases. Also, geological situations are generally more complex than these assumptions, and solutions cannot be generally regarded as unique. However, the curves should help in devising first approximations to interpretation and in deciding what departures from the ideal case are likely.

Parameters have been calculated and plotted to assist in identification of dip angle and depth ratio. When these have been identified, the actual dimensions, location, and density contrast of the structure can be obtained from a series of graphs, or in the case of the logarithmic curves, by direct reading on the logarithmic co-ordinate scales.

1. INTRODUCTION

It is well known that, for geophysical measurements of physical quantities derived from potential functions, there is in general no unique solution in terms of underground structure. However, in many cases, other information leads to restrictions on the range of possible solutions and enables a reasonable approximation to be made.

One approach commonly used in interpretation is to assume various simple geometrical shapes for the anomalous body and to calculate the corresponding anomaly, which is compared with the observed curves. Sometimes sets of standard curves are prepared, so that if the assumption is made that the anomalous body has a given shape, a unique solution can be obtained by matching the observed anomaly against one of the standard curves.

The simple shape assumed probably does not represent the geological reality accurately. Such interpretations are nevertheless useful as a guide to the general possibilities and may place some limits on the solution. They may also suggest in what way the actual anomalous body departs from the assumed shape. In general, for a first interpretation or where other evidence is lacking, the simplest hypothesis that is geologically and physically plausible should be tried as a first solution; complications should be introduced only insofar as there is evidence for them.

The step-like gravity anomaly generally associated with a fault, in which the gravity values change from one area of more or less uniform gravity values to another area of uniform but different gravity values, the two areas being separated by a gradient of parallel contour lines, is one that occurs commonly and is most readily interpreted in general terms. The usual first interpretation is by approximation to a thin horizontal semi-infinite plate (e.g. Nettleton, 1942). However, this is inaccurate if the fault or contact plane approaches the surface.

The next complications in this interpretation are to ascribe finite thickness to the anomalous layer on one side of the contact plane and to permit the contact plane to dip at an angle other than vertical. The first alters the shape of the gravity anomaly curve somewhat, but it remains symmetrical about the contact plane; the second leads to an asymmetrical curve.

The formula for the gravity anomaly of a sloping contact is given by Heiland (1946, p 153). Jung (1927) prepared a set of diagrams for determining the depth and dip of a slope based on gravity gradients and curvatures as measured with a torsion balance. Chastenet de Géry and Naudy (1957) have prepared logarithmic curves for interpreting a vertical fault of finite thickness in terms of the vertical gradient of gravity.

In this paper, a series of gravity anomaly profiles is calculated for the general case of a sloping contact between two semi-infinite horizontal slabs of uniform density contrast.

Although the formulae for vertical gradient and second derivative have certain advantages in interpretation, there are reasons for preferring a comparison of the directly observed quantities with theoretical curves. Calculation of the derivatives is done by numerical procedures involving the observations to a considerable distance from the point being considered, and any small errors or irregularities in the observations are magnified by these procedures. Although the derivatives, profiles, or contours may make certain information more obvious, the information is necessarily present in the original observations, and no numerical manipulation can make it any more reliable.

Some smoothing or elimination of regional effects may be necessary before making a comparison with the standard curves; this is discussed later. Otherwise, the only treatment of observed data is the choice of calibration factor and origin of co-ordinates to enable comparison with the standard curves, and the scaling of ordinates from the plotted profile.

The computations were programmed for the Ferranti Sirius computer. Anomaly profiles were computed for various angles of dip and for various depths to the top of the slope, the depth to the bottom of the slope being taken as unit distance. Parameters could then be scaled from the profiles and used to identify the dip and depth of the anomalous body. Other dimensions required for the complete solution are given in graphs.

2. THEORY

Let us consider first the case where the fault crops out (Figure 1). Let the angle of dip be ϕ ($0 < \phi < \pi/2$ for a normal fault; $\pi/2 < \phi < \pi$ for a reverse or overthrust fault), and the depth to the basement at the foot of the fault be z_o. We shall calculate the anomaly at the point P, which is taken as the origin of co-ordinates x and z (x positive to the right, z positive downwards). The basement below depth z_o may be ignored, as this contributes uniformly to the gravity field, and the anomaly due to the fault is the same as that due to the chisel-shaped layer A_i (i = 1, 2, 3, 4) where A_2 and A_3 are at infinity. Let the co-ordinates of A_i be (x_i, z_i) and let the angle between the x axis and the line PA_i be θ_i. Let the angle between the x axis and A_iA_{i+1} be ϕ_i, measured clockwise from the x axis. The co-ordinates etc. of the points A_i are given in tabular form below.

i	x_i	z_i	θ_i	ϕ_i
1	d	0	π (d negative) 0 (d positive)	0
2	∞	0	0	-
3	∞	z_o	0	0
4	$d - z_o \cot \phi$	z_o	$\text{arcot} (d/z_o - \cot \phi)$	$\pi - \phi$

The anomaly is obtained from the formula for an extended body of polygonal cross-section given by Talwani, Worzel, and Landisman (1959). The anomaly is given by

$$2 \Delta\rho k \sum_{i=1}^{4} v_i$$

where v_i corresponds to Z_i of Talwani et al (loc. cit.), k is the gravitational constant, and $\Delta\rho$ the density contrast.

From Case C of Talwani et al,

$$v_1 = 0$$

From Case E,

$$v_2 = 0$$

From Case C,

$$v_3 = z_o(\theta_4 - \theta_3) = z_o \text{ arcot} (d/z_o - \cot \phi)$$

For v_4, we use the general expression, but A_{i+1} becomes A_1 instead of A_5 in order to complete the cyclic summation, and the a_i of Talwani et al becomes equal to d.

$$v_4 = d \sin \phi_4 \cos \phi_4 \left[\theta_4 - \theta_1 + \tan \phi_4 \log_e \frac{\cos \theta_4 (\tan \theta_4 - \tan \phi_4)}{\cos \theta_1 (\tan \theta_1 - \tan \phi_4)} \right] \quad \ldots\ldots\ldots (1)$$

The argument of the logarithmic function can be put in a more convenient form by substituting for θ_1 and ϕ_4 from the table. We get

$$\cos\theta_4 (\tan\theta_4 + \tan\phi)/\tan\phi = \sin\theta_4 (\cot\phi + \cot\theta_4)$$

$$= d\sin\theta_4/z_o$$

$$= (d/z_o)\left[1 + (d/z_o - \cot\phi)^2\right]^{-\frac{1}{2}}$$

To avoid separate discussion of the cases for d positive and negative, we may write $\theta_1 = H(-d)\pi$, where $H(y)$ is the Heaviside function, defined as zero for $y < 0$ and 1 for $y > 0$. Then we have:

$$v_4 = H(-d)\pi d \sin\phi \cos\phi - d\sin\phi \cos\phi \operatorname{arcot}(d/z_o - \cot\phi)$$
$$- \tfrac{1}{2}d\sin^2\phi \log_e\left[(z_o/d)^2 + (1 - z_o\cot\phi/d)^2\right] \quad\ldots\ldots(2)$$

The anomaly is then given by $2k\Delta\rho v_o$, where

$$v_o = v_3 + v_4$$

$$= H(-d)\pi d \sin\phi \cos\phi + (z_o - d\sin\phi \cos\phi)$$
$$\operatorname{arcot}(d/z_o - \cot\phi)$$
$$-\tfrac{1}{2}d\sin^2\phi \log_e\left[(z_o/d)^2 + (1 - z_o\cot\phi/d)^2\right]$$
$$\quad\ldots\ldots(3)$$

which may also be written

$$v_o = H(-d)\pi d \sin\phi \cos\phi + (z_o - d\sin\phi \cos\phi)\theta_4$$
$$- \tfrac{1}{2} d\sin^2\phi \log_e(r^2/d^2), \quad\ldots\ldots(4)$$

where $r = \left[z_o^2 + (d - z_o\cot\phi)^2\right]^{\frac{1}{2}}$ is the distance PA_4 in Figure 1.

As d becomes large positively, neglecting second order terms,

$$\theta_4 \rightarrow z_o/(d - z_o\cot\phi)$$

and the second term in equation (3) approaches

$$\frac{z_o(z_o - d\sin\phi \cos\phi)}{d - z_o\cot\phi} = \frac{z_o(z_o/d - \sin\phi \cos\phi)}{1 - z_o\cot\phi/d}$$

$$\longrightarrow - z_o\sin\phi \cos\phi$$

Further,

$$r^2/d^2 = 1 - 2z_o\cot\phi/d + z_o\operatorname{cosec}^2\phi/d^2$$

and neglecting second-order terms, as d becomes large,

$$\log_e(r^2/d^2) \longrightarrow - 2z_o\cot\phi/d$$

Thus the third term approaches

$$z_o\cot\phi \sin^2\phi = z_o\cos\phi \sin\phi.$$

Therefore, $v_o \longrightarrow 0$ as $d \longrightarrow +\infty$.

As $d \longrightarrow -\infty$, the third term in equation (3) again approaches $z_o\cos\phi \sin\phi$. The first two terms approach

$$\pi d \sin\phi \cos\phi + (z_o - d\sin\phi \cos\phi)\left(\pi + \frac{z_o}{d - z_o\cot\phi}\right)$$
$$\longrightarrow \pi z_o - z_o\sin\phi \cos\phi.$$

Thus, $v_o \longrightarrow \pi z_o$

Let us now transform the co-ordinates such that A_1 is origin and z_0 is taken as unit of length. Then the co-ordinate of P in the new system is

$$D = - d/z_0 \qquad \ldots\ldots\ldots\ldots(5)$$

Let us further normalise the anomaly so that it ranges from -1 (at $D = -\infty$) to $+1$ (at $D = +\infty$). Let the normalised anomaly be G_0. Then

$$G_0 = \frac{2 v_0}{\pi z_0} - 1 \qquad \ldots\ldots\ldots\ldots(6)$$

$$= - H(D) \, 2 \, D \sin \phi \cos \phi + (1 + D \sin \phi \cos \phi) \, 2 \, \theta/\pi$$
$$+ D/\pi \sin^2 \phi \, \log_e (R^2/D^2) - 1, \qquad \ldots\ldots\ldots\ldots(7)$$

where $R = r/z_0 = \left[1 + (D + \cot \phi)^2 \right]^{\frac{1}{2}}$

and $\cot \theta = - D - \cot \phi.$

For a reverse slope ($\phi > \pi/2$), Figure 1 would apply if $\Delta\rho$ was negative. The anomaly would be changed in sign from the normal case, and no separate treatment is necessary. The curve is the reverse of that obtained for $\pi - \phi$.

Let us now consider the case where the slope does not reach the surface, but is truncated by a horizontal plane at depth z_1 (Figure 2.) (Note that z_1 as defined here is different from $z_1 = 0$ of the table on page 2.) The anomaly may be considered as the difference between two outcropping wedges $A_1 A_2 A_3 A_4$ and $A_1 A_2 A_5 A_6$, with thicknesses z_0 and z_1 respectively.

From equation (3), we see that v_0/z_0 may be written as a function of d/z_0 and ϕ only; from equation (6) this may be put in the form

$$v_0/z_0 = \pi/2 \left[1 + G_0(\phi, \, d/z_0) \right]$$
$$= \pi/2 \left[1 + G_0(\phi, \, D) \right]$$

Similarly for the upper wedge,

$$v_0^1/z_1 = \pi/2 \left[1 + G_0 (\phi, \, d/z_1) \right]$$

Putting $Z_1 = z_1/z_0$, this becomes

$$v_0^1/z_0 = Z_1 \, \pi/2 \left[1 + G_0 (\phi, \, D/Z_1) \right]$$

Thus, $(v_0 - v_0^1)/z_0 = \pi/2 \left[(1 - Z_1) + G_0 (\phi, \, D) - Z_1 \, G_0 (\phi, \, D/Z_1) \right]$

This ranges from $(\pi/2 - 1) (1 - Z_1)$ to $(\pi/2 + 1) (1 - Z_1)$

Therefore, to obtain a normalised anomaly G with the same range as G_0, divide by $(1 - Z_1)\pi/2$ and subtract 1, i.e.

$$G(\phi, \, D, \, Z_1) = \frac{G_0 (\phi, \, D) - Z_1 \, G_0 (\phi, \, D/Z_1)}{(1 - Z_1)} \qquad \ldots\ldots\ldots\ldots(8)$$

3. COMPUTATIONAL PROCEDURE

The procedure used was to calculate G_0 from equation (7) as a function of D for various angles of dip $\phi = 5^0$, 10^0, 15^0, 30^0, 45^0, 60^0, 75^0, 90^0.

Let us now write

$$b = D \sin \phi \cos \phi$$

$$w = \tfrac{1}{2} D \sin^2 \phi \log_e (R^2/D^2)$$

and put equation (7) in the form

$$G_0 = 2 (u + w)/\pi$$

For actual computation it is necessary to consider three cases. The Ferranti Sirius computer always interprets inverse trigonometric functions as an angle between $-\pi/2$ and $+\pi/2$. In our notation, the range of θ is from 0 to π; if $D > -\cot \phi$, $\cot \theta$ is negative and will be interpreted by the machine as $\theta^1 = \theta - \pi$

Case 1. $D < -\cot \phi$, $\cot \theta > 0$

$$u = (1 + b) \theta - \pi/2$$

Case 2. $0 > D > -\cot \phi$, $\cot \theta < 0$

$$u = (1 + b) (\theta^1 + \pi) - \pi/2 = \pi/2 + \theta^1 + b (\pi + \theta^1).$$

Case 3. $D > 0$, $\cot \theta < 0$

$$u = -\pi b + (1 + b) (\theta^1 + \pi) - \pi/2$$

$$= (1 + b) \theta^1 + \pi/2$$

The programme must test for these three cases and calculate u accordingly.

For depths to the top surface other than zero, G was calculated for various values of z_1 from equation (8).

In order to use equation (8), it is necessary that G_0 should be calculated for corresponding values of D and D/z_1. This was achieved by using logarithmic increments in the values of D selected for computation of $G_0(D)$. Z_1 was then selected so that D/Z_1 was an exact number of increments from D throughout its range. The increment used was $\log_{10} (D_{n+1}/D_n) = 0.1$, so that

$$D_{n+1} = 1.2589 D_n$$

D_1 was put equal to ± 0.01, and the calculations were carried out to 50 increments, i.e. to $D = \pm 1,000$. Values of Z_1 were chosen so that

$$\log_{10} (1/Z_1) = 0.1, 0.3, 0.5, 0.7 \text{ and } 1.0$$

corresponding to

$$Z_1 = 0.7943, 0.5012, 0.3162, 0.1995, 0.1000$$

$$\approx 0.8, 0.5, 0.32, 0.2, 0.1$$

Thus, the effective range of D was smallest for $Z_1 = 0.1$, in which case it was ± 100.

The curves for G as a function of D are plotted in Figures 3 and 4. In the limiting case, as $Z_1 \to 1$, the anomaly curve approaches that for an infinitely thin sheet (Nettleton, 1940, p. 113). The normalised anomaly for this case is

$$G_1 = \frac{2 \, \text{artan} \, (D + \cot \phi)}{\pi} \qquad \dots\dots\dots\dots(9)$$

This curve is the same shape for all values of ϕ and is symmetrical about $D = -\cot \phi$, where $G_1 = 0$. G_1 has been plotted with the other curves.

One point of interest is that for a given value of ϕ, all the curves pass through the same point at $D = 0$. At this point, $\theta_4 = \pi - \phi$, and from equation (7) it may be seen that

$$G_o = 1 - 2\phi/\pi \qquad \dots\dots\dots\dots(10)$$

It will be noticed that the curves have a sharper curvature above the upper vertex of the fault than above the lower vertex. With a reverse slope or overthrust fault, the sharper curvature occurs in the lower part of the curve, and this is a guide to distinguishing the two cases, as has been pointed out by Bott (1961) and Romberg (1958). As Z_1 increases, the asymmetrical features diminish.

Another advantage of the logarithmic increments is that more values are calculated near the origin, where G changes more rapidly, than for high values of D. Actually, for small angles of dip, the maximum gradient is displaced considerably from the origin, and the small starting value of $D = .01$ was necessary to accommodate this.

The values of G were generally calculated for more points than necessary (a) near the origin, where D increments were small, and (b) for large values of D, where $G \to \pm 1$. As the main factor determining machine time was the punching out of results, the programme was devised so that answers were printed out only when G increased numerically by 0.02 or more from the previous value. Thus the first value of G to exceed 0.98 would be the last one printed out.

In order to facilitate direct interpretation of anomaly curves, it is necessary to work with parameters that can be determined from the curves themselves. In general, the location of the origin of co-ordinates ϕ, z_o, and z_1 will be unknown, and the problem is to determine these from the observed curve.

Let the observed anomaly profile be $g(x)$, where x is the horizontal distance at right angles to the gravity contours, and g and x have arbitrary datums. Let g tend to g_2 and g_1 as $x \to \pm \infty$ (Figure 2). Then, by putting

$$G' = \frac{g(x) - (g_2 + g_1)/2}{(g_2 - g_1)/2} = \frac{2g(x) - (g_2 + g_1)}{(g_2 - g_1)} \qquad \dots\dots\dots\dots(11)$$

we get a function ranging from -1 to $+1$, similar to G (D) (see Figure 2). We can determine graphically the values of x corresponding to various values of G'; let these be $x(G')$. We now transform the x co-ordinates so that

$$X(G') = \frac{x(G') - x(0)}{x(.5) - x(-.5)} \qquad \dots\dots\dots\dots(12)$$

The problem is to find the relation between X and D, such that G' (X) and G(D) are as close as possible. There is no simple algebraic solution in general for equations (3) and (8) to determine D (G) for selected values of G. Therefore the equations must be solved by numerical processes.

Solutions were obtained by an iterative interpolation procedure for D (0), D ($\pm$ .5), D ($\pm$ .25), and D ($\pm$ .75), for each curve of G. Values of X were then calculated as in equation (12):

$$X (G') = \frac{D(G) - D(0)}{D(.5) - D(-.5)} \qquad \dots\dots\dots\dots(13)$$

These were obtained for the solved values of X ($\pm$ .5), X ($\pm$ .25) and X ($\pm$ .75) for use as parameters in direct solution. The solutions are plotted in Figure 5 as functions of $\emptyset$ for various values of Z. Values of X were also calculated for all values of D printed out, thus enabling anomaly curves to be drawn normalised in terms of the curve parameters, for comparison with similar normalised curves obtained by equations (11) and (12) from observed anomaly curves. These curves G'(X) are plotted in Figures 6 to 13. They are also plotted with logarithmic scales in Figures 14 to 21. As described later, the co-ordinates of the logarithmic curves have been modified.

Further parameters calculated were

$$S (G) = X (G) - X (-G) \qquad \dots\dots\dots\dots(14)$$

$$T (G) = X (G) + X (-G) \qquad \dots\dots\dots\dots(15)$$

giving S (.25), S (.75), T (.25), T (.5), and T (.75). Of course S (.5) is 1.0 by definition.

Of these, the T parameters are indications of asymmetry in the curve, S (.25) indicates the gradient near the centre, and S (.75) the rate of approach to the asymptotes in the outer parts. The S and T parameters are plotted as functions of $\emptyset$ for various values of Z_1 in Figure 22. Contours of equal values of $\emptyset$ and Z_1 have been plotted in Figure 23 using various pairs of S and T parameters as co-ordinates.

Other parameters required in the interpretation (see Figure 2) were calculated as follows;

$$z_0/x_1 = 1/ \left[D (.5) - D (-.5) \right] \qquad \dots\dots\dots\dots(16)$$

$$z_1/x_1 = Z_1 \, z_0/x_1 \qquad \dots\dots\dots\dots(17)$$

$$z_m/x_1 = (z_0 + z_1)/2 \, x_1 \qquad \dots\dots\dots\dots(18)$$

$$\Delta z / x_1 = (z_0 - z_1)/x_1 \qquad \dots\dots\dots\dots(19)$$

$$Z_m = (1 + Z_1)/2$$

$$X_m = \frac{Z_m \cot \emptyset + D (0)}{D (+.5) - D (-.5)} \qquad \dots\dots\dots\dots(20)$$

In these equations, x_1 is the distance between the points at which G' = $\pm$ 0.5, as scaled from the observed curve. The suffix m refers to co-ordinates of the mid-point of the slope. The functions defined by equations (16) to (20) have been plotted in Figures 24 and 25.

4. INTERPRETATION PROCEDURE

The curve G from equation (8) is a function of ϕ, Z_1, and D only. The graphs of the S and T parameters (Figures 22 and 23) show that appropriate pairs of these, if determined accurately enough, are sufficient to determine ϕ and Z_1 completely. It follows that ϕ and Z_1 can also be determined by matching the normalised observed curve against the theoretical curves.

In practice, the interpreted results may be wrong because of several factors, such as:

(a) The model may be too simple - i.e. the density contrast may vary, or may occur across more than one surface; the surface may be curved or change slope; the assumption of infinite extension of the profile at right angles to the section line may not be justified.

(b) Gravity observations may not be accurate enough or they may be spaced too far apart.

(c) Other sources of gravity variations may be difficult to eliminate.

If other information is available, e.g. geological mapping, drilling, seismic or magnetic measurements, or density measurements of rock samples, some of the parameters may be determined independently and the interpretation improved accordingly. However, in the absence of such information it is probably best to aim at the simplest interpretation.

Several possible procedures will be described under the following headings:

1. Use of S and T parameters.

2. Matching of normalised curve.

3. Matching of logarithmic curve.

4. Special cases.

Whatever method is used, it will probably be necessary to carry out some smoothing to eliminate local irregularities or to eliminate regional trends. While various automatic methods of calculating residual features are sometimes used, it is probably better for the interpreter to use his judgement in smoothing, particularly if he suspects the nature of the interfering sources. The residuals or regionals calculated by automatic procedures are unlikely to correspond to anomalies traceable to real sources; thus it might be misleading to make a quantitative interpretation of the remaining anomaly. With smoothing by hand the danger is also present of course, but it is easier to judge the inaccuracies in the discarded portion of the anomaly, or to vary the amount discarded and to check the effect of this on the interpretation.

Method 1 - Use of S and T parameters

Having drawn a suitably smoothed curve, it is first necessary to decide on the asymptotic values g_1 and g_2. This may be difficult if disturbing anomalies exist near the fault; it can be seen from the curves in Figures 6 to 21 that in some cases the asymptotic value is not approached within a few percent until X is between about 5 and 10. A generous allowance should be made for the 'tailing off' part of the curve if it cannot be plotted to considerable distances. We then take X = 0 at $g = \frac{1}{2}(g_1 + g_2)$, and scale off x from equation (11) for $G' = \pm .5, \pm .25, \pm .75$, and calculate the corresponding values of X from equation (12).

If the curve appears to be symmetrical, the origin of the X and G' co-ordinates may be chosen at the maximum gradient, or half-way between points of equal curvature if g_1 and g_2 cannot be determined accurately.

The S and T parameters are then determined from equations (13), (14), and (15). One of the nomograms in Figure 23 should be chosen such that the S and T parameters give good resolution, and ϕ and Z_1 should be determined from the nearest curves passing this point.

It is obvious that for small values of T when $S\,(.75) \approx 2.4$ or $S\,(.25) \approx .43$ the resolution will be poor. If the S values depart substantially from the above, it will be possible to distinguish between a steeply dipping (almost vertical) and comparatively shallow fault, e.g. when $S\,(.75) > 2.4$ and $S\,(.25) < .43$, and a deeper incline of small angle, e.g. when $S\,(.75) < 2.4$ and $S\,(.25) > .43$.

Having determined ϕ and Z_1 from one pair of parameters, it is wise to check that the other parameters are consistent with this interpretation. This could be perhaps best done by checking the X values on the graphs in Figure 5. If there are any discrepancies, the X values would give the most direct indication of the way in which the curve departs from a standard curve, leading to suggestions for a change of co-ordinates, variation in the smoothing procedure, or an additional source of anomalies that might explain the departure.

Having arrived at satisfactory values of ϕ and Z_1, we can determine z_0/x_1, z_1/x_1, z_m/x_1, $\Delta z/x_1$, and X_m from the graphs in Figures 24 and 25. The dimensions and location of the sloping boundary can be calculated by multiplying these quantities by x_1.

As a further aid to interpretation, the portion of each anomaly curve that is immediately above the sloping surface is drawn in a heavier line in Figures 3 and 4 and Figures 6 to 21. Thus, the ends of the heavy lines in Figures 6 to 12 give X_a and X_b (Figure 2). For $\phi = 90°$, of course, $X_a = X_b = 0$, and no heavy lines appear.

The density contrast may then be calculated from

$$\Delta \rho = (g_2 - g_1)/2 \pi k \Delta z \qquad \ldots\ldots\ldots(21)$$

Method 2 - Matching of normalised curves

The initial procedure is to fix the origin of the X and G' co-ordinates as in method 1. Having done this, X and G' are calculated for all observation points (or for the corresponding smoothed values) from equations (11) and (12), and a curve is drawn on the same scale as the standard curves. This is matched to the best fitting standard curve, which will give values of Z_1 and ϕ.

As this involves fitting the curve throughout, it might give a better result than method 1, and would almost certainly give a better idea of departures and their possible causes, particularly if these involved small changes of origin or a systematic calibration-factor deviation. However, there is more work in drawing such a curve, and it might be best to use method 1 initially to gain some idea of the parameters, and make adjustments if necessary before drawing the curve. The curve-fitting would be a desirable check after using method 1.

Method 3 - Matching of logarithmic curves

Curves with double-logarithmic scales have been used for fitting many geophysically observed curves, e.g. in resistivity depth probing, gravity, and vertical gradients of gravity (Chastenet de Géry and Naudy, 1957; Naudy, 1962).

The advantage is that the results can be plotted directly from the field observations without change of unit; however, choice of origin is important. In most cases where this method is used, the origin is obvious, but there are difficulties in locating it precisely in the present case. A small error in origin may cause a large change in the appearance of the curve, particularly for small values of G' and X. For this reason, it may generally be better to use the curves with linear co-ordinates as in method 2, unless the position of the origin is fairly certain.

However, because of the convenience of plotting the logarithmic curves and because the parameters can be determined directly, in some cases it may be worthwhile selecting several origins within the probable range of origins, and trying to match the curves based on each of these.

First the position of the origin must be estimated as in method 1 and the values of g_0 and x_0 subtracted from g and x respectively. The logarithmic curves may then be plotted in units as measured, multiplied by convenient powers of 10. The two branches of the curve (negative and positive) must be plotted separately, as the origin ($G' = 0$, $X = 0$) is at $-\infty$. For the master curves (Figures 14 to 21), the branches have been plotted on the same co-ordinate system; for the negative branch the positive quantities $-X$ and $-G'$ have been plotted. The observations should be plotted similarly and laid over the master curves until the pair of curves is found whose two branches best fit the observations. The separation of the branches should fit as well as their shapes. ϕ and Z_1 are obtained by identification of the best fitting curves.

The master curves were first plotted as X, G' curves, and they were then displaced vertically by a distance of $\log x_1/z_0$, and horizontally by $\log \triangle Z$ (see Figure 26). Thus the co-ordinate scales in Figures 14 to 21 are $(x - x_0)/z_0$ and $G' \triangle Z$. The displaced "origins" ($X = 1$, $G' = 0.1$) are indicated by crosses. Let O be the intersection of the axes $(1,1)$ on the master curve adopted as best fitting the observations. Then, when the observations are superimposed on the curve, the co-ordinates of O on the scale of the observations are z_0 and $(g_2 - g_1)/2\triangle Z$ (Figure 26). (As some of the curves overlap substantially in spite of the displacement of origin, in some cases alternate curves have been plotted with a further vertical displacement corresponding to a factor of 10 for the sake of clarity).

From equation (21), the latter expression is the same as $\pi k z_0 \triangle \rho$. We take k as 6.673×10^{-8} cgs units (Heiskanen and Vening Meinesz, 1958, p. 156). If z is measured in kilometres, g in milligals, and ρ in g/cm^3, then we have $\pi k = 20.96$. To get $\triangle \rho$, we therefore need to divide the above expression by $20.96 z_0$. This may be done in a manner similar to a slide rule calculation on a convenient vertical axis of the observations co-ordinate system. To divide by 20.96, we measure a distance of $\log 20.96$ below the origin of the standard curve; to facilitate this, a mark is made at a point P (Figure 26) on the unit vertical axis of each set of standard curves, at $G \triangle Z = 1/20.96 = 0.0477$. The horizontal distance of P from the vertical axis through $x - x_0 = 1$ kilometre is $\log z_0$ (z_0 in kilometres). Thus a line drawn through P at $45°$ to the axes will intersect the 1-kilometre axis at a point $\log z_0$ below P, and the co-ordinate of this point on the logarithmic milligal scale of observations will give $\triangle \rho$ in g/cm^3 (Figure 26).

Parallel lines have also been drawn through points at $G \triangle Z = 3.281 \times 0.0477 = 0.1565$, and at $G \triangle Z = 0.6214 \times 0.0477 = 0.02964$; the intersections of these with the vertical axes $x - x_0 = 1000$ ft or 1 mile respectively will give $\triangle \rho$ in g/cm^3. Axes through decimal multiples or sub-multiples of these distances can also readily be used to obtain $\triangle \rho$; e.g., if the 1-kilometre, 45-degree line cuts the axis $x - x_0 = 10^n$ km at $G \triangle Z = p$, then $\triangle \rho$ is given by $10^{-n}p$.

As with the linear curves, the portion of each logarithmic master curve (Figures 14 to 21) located above the sloping surface is drawn in a heavier line. When the master curve is superimposed on the observations, the ends of the heavy lines give x_a and x_b (Figure 2) directly on the horizontal distance scale of the observations (see Figure 26). With some curves, the ends of the heavy lines are off scale; in these cases the points corresponding to $10\ x_a$ and $10\ x_b$ have been marked on the curves.

Special cases

The vertical fault ($\phi = 90^{\circ}$). This has been discussed by Bancroft (1960). An exact analytical solution can be obtained for the maximum gradient of G in terms of Z_1.

In this case, equation (7) simplifies to

$$G_o = (2/\pi)\ \text{artan}\ D + (D/\pi)\ \log_e (1 + 1/D^2)$$

and equation (8) becomes

$$G = \frac{2}{\pi(1-Z_1)} \left[\text{artan}\ D - Z_1\ \text{artan}\ D/Z_1 + \tfrac{1}{2}D \log_e \left(\frac{D^2 + 1}{D^2 + Z_1{}^2}\right)\right]$$

$$U = \frac{d\ G}{d\ D} = \frac{1}{\pi(1-Z_1)}\ \log_e \frac{D^2 + 1}{D^2 + Z_1{}^2} \qquad \ldots\ldots\ldots(22)$$

U is a maximum (U_o) when $D = 0$ ($Z_1 < 1$), i.e.

$$U_o = 2 \log_e (1/Z_1)/\pi(1-Z_1) \qquad \ldots\ldots\ldots(23)$$

Note that for $Z_1 = 0$, U_o becomes infinite. Thus for outcropping or nearly outcropping vertical faults, the gradient is very steep immediately over the fault, as may be seen in the X, G curve for $\phi = 90^{\circ}$, $Z_1 = 0$ (Figure 13).

The outcropping fault plane. If the outcrop can be traced on the surface, then we can obtain ϕ from equations (10) and (11):

$$\tfrac{1}{2}(1-G_s) = \phi/\pi = \tfrac{1}{2}(1-G'_s) = (g_2 - g_s)/(g_2 - g_1), \qquad \ldots\ldots\ldots(24)$$

where g_s is the value of g (X) at the outcrop, and G_s and G'_s the corresponding values of G and G'.

Note that this equation holds even if $Z_1 \neq 0$, i.e. if the effective density contrast does not reach the surface. Thus the sum of the anomalies due to a series of density contrasts across the same dipping plane would also obey equation (24). By taking the sum of the effect of a large number of very thin plates, it can be shown that equation (24) holds for a density contrast that may vary continuously or discontinuously with depth, provided only that the density contrast in any horizontal band occurs across the one sloping plane; or in other words, that density on either side of the sloping plane is a function of depth only.

If it can be assumed that the density contrast across the sloping plane is uniform, and presumably extends to the surface if the contact can be mapped in outcrop, then $Z_1 = 0$, and the other parameters can be calculated as before.

In this case, there are some restrictions on the form the curve can take, and these can help in the interpretation, in checking whether a simple slope can give an adequate interpretation.

Parameters derived from other sources. An estimate of ΔZ may sometimes be made from drilling or seismic work, or $\Delta\rho$ may be known from measurements of rock samples. In either case, the other one can be calculated from equation (21). Again, this information limits the possible curves and enables a check to be made on the interpretation.

In general, the parameters derived from any interpretation should of course be checked against any other geological or geophysical knowledge in the area and for their inherent reasonableness.

Anomalies involving more than one slope. The anomaly curves (Figures 3 and 4) can be used to build up profiles of bodies of more complicated cross-section, involving sides with various slopes. A unique interpretation would not generally be possible if more than one sloping surface is required to explain the anomaly. If more than two or three slopes are involved it would probably be better to compute the anomaly for supposed profiles, either graphically or by digital computer (e.g. Talwani et al, 1959)

13.

REFERENCES

BANCROFT, A.M. — 1960 — Gravity anomalies over a buried step. _J. Geophys. Research_, 65 (5), 1630-1631.

BOTT, M.H.P. — 1961 — Quoted in "Interpretation of geophysical surveys." _Nature_, 192 (4809), 1242-1243.

CHASTENET DE GÉRY, J. and NAUDY, H. — 1957 — Sur L' interprétation des anomalies gravimétriques et magnétiques. _Geophys. Prosp._, 5, p. 421-448.

HEILAND, C.A. — 1946 — GEOPHYSICAL EXPLORATION New York, Prentice-Hall Inc.

HEISKANEN, W.A. and VENING MEINESZ, F.A. — 1958 — THE EARTH AND ITS GRAVITY FIELD New York, McGraw-Hill Book Co. Inc.

JUNG, K. — 1927 — _Zeit. Geophys._ 3 (6), 267-280.

NAUDY, H. — 1962 — Contribution des abaques bilogarithmiques a l'interprétation gravimétrique. _Geophys. Prosp._ 10 (2), 171-176.

NETTLETON, L.L. — 1940 — GEOPHYSICAL PROSPECTING FOR OIL. New York, McGraw-Hill Book Co. Inc.

NETTLETON, L.L. — 1942 — Gravity and magnetic calculations. _Geophysics_, 7 (3), 293-310.

ROMBERG, F.E. — 1958 — Key variables of gravity. _Geophysics_, 23 (4), 684-700.

TALWANI, M., WORZEL, J.L., and LANDISMAN, M. — 1959 — Rapid gravity computations for two dimensional bodies with application to the Mendocino submarine fracture zone. _J. Geophys. Research_, 64 (1), 49-59.

FIG. I

FIGURE 1
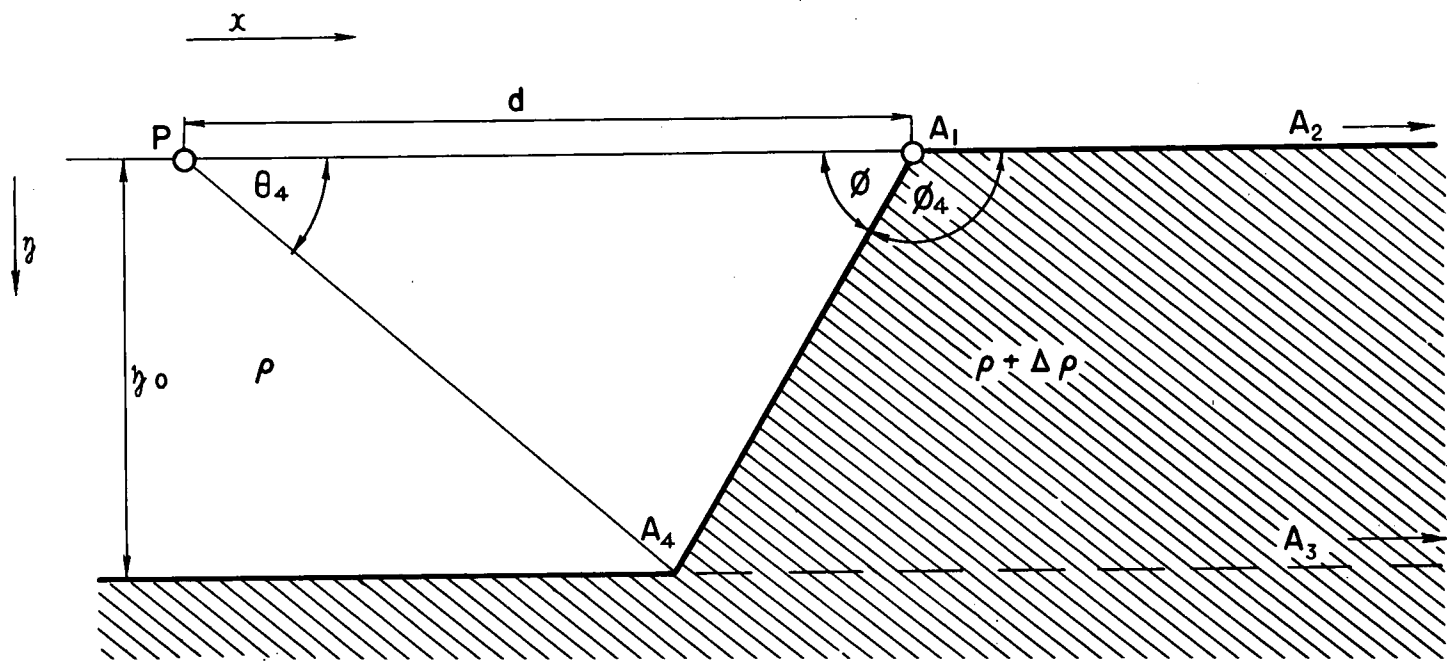
FIG.I   OUTCROPPING   SLOPING   CONTACT
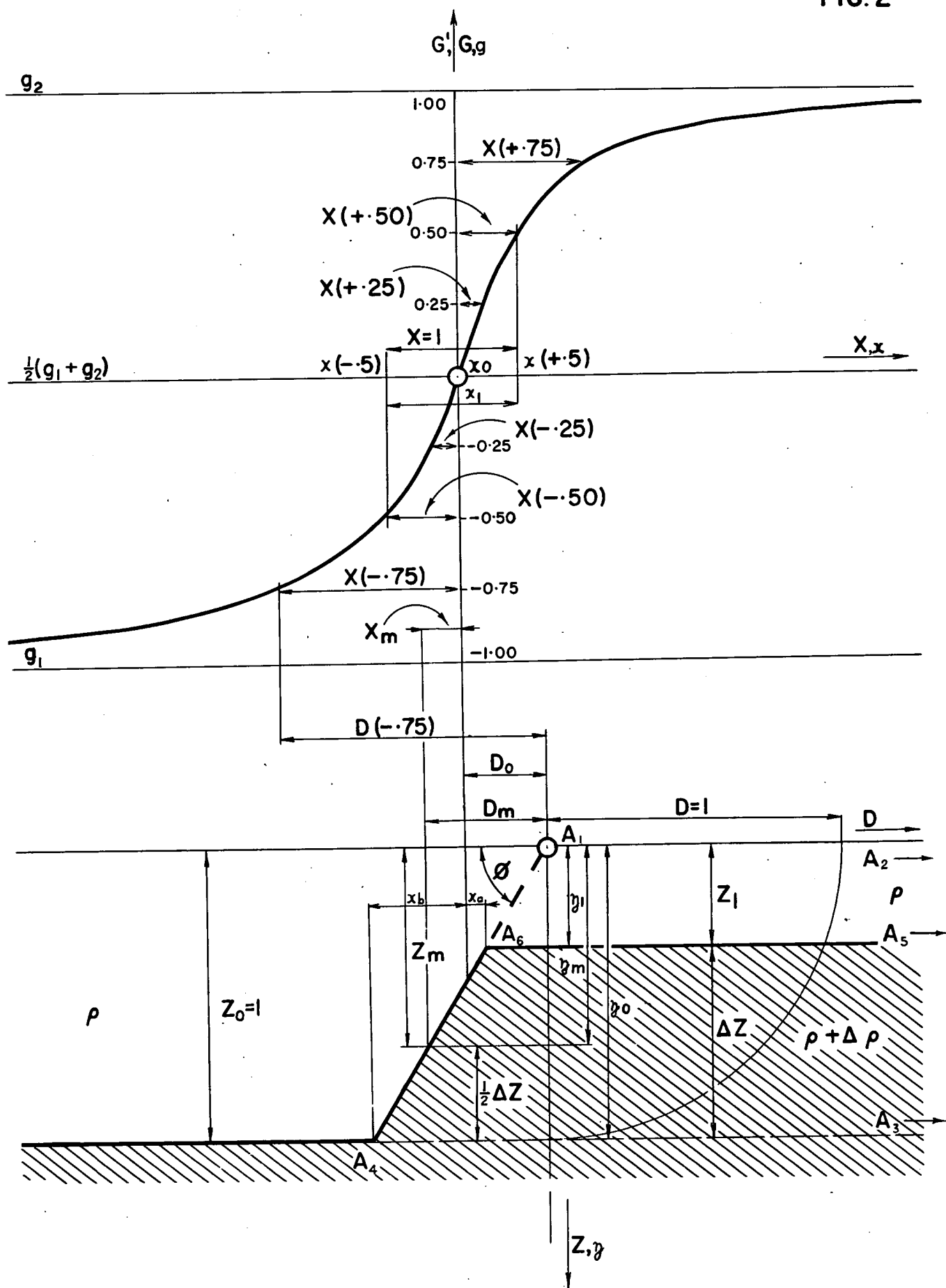
FIG. 2

ACTUAL CO-ORDINATES (lower case letters) AND

NORMALISED CO-ORDINATES (CAPITALS)
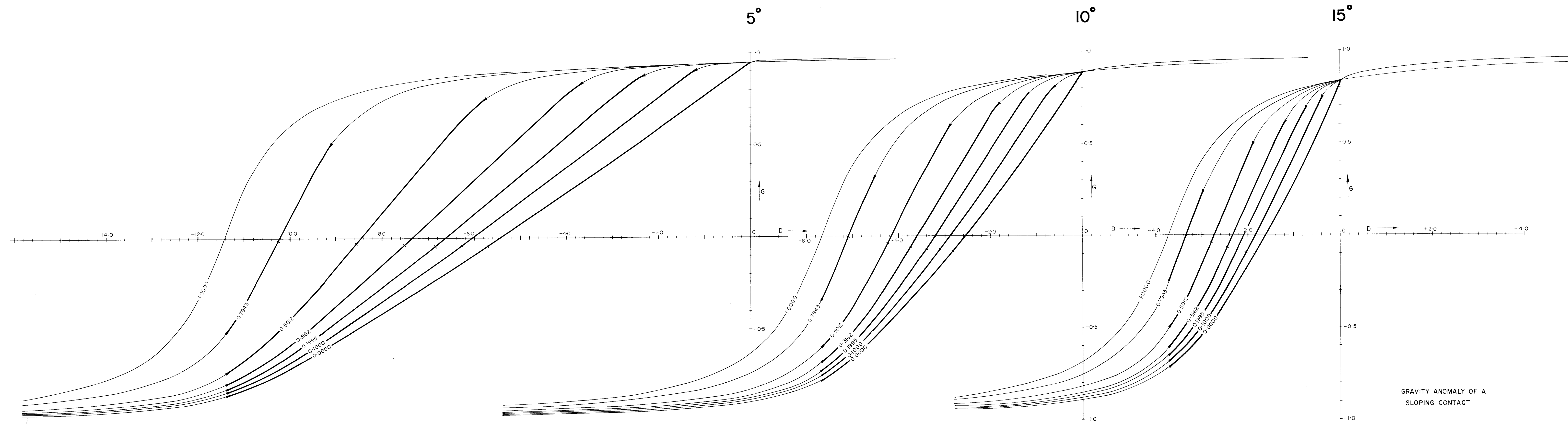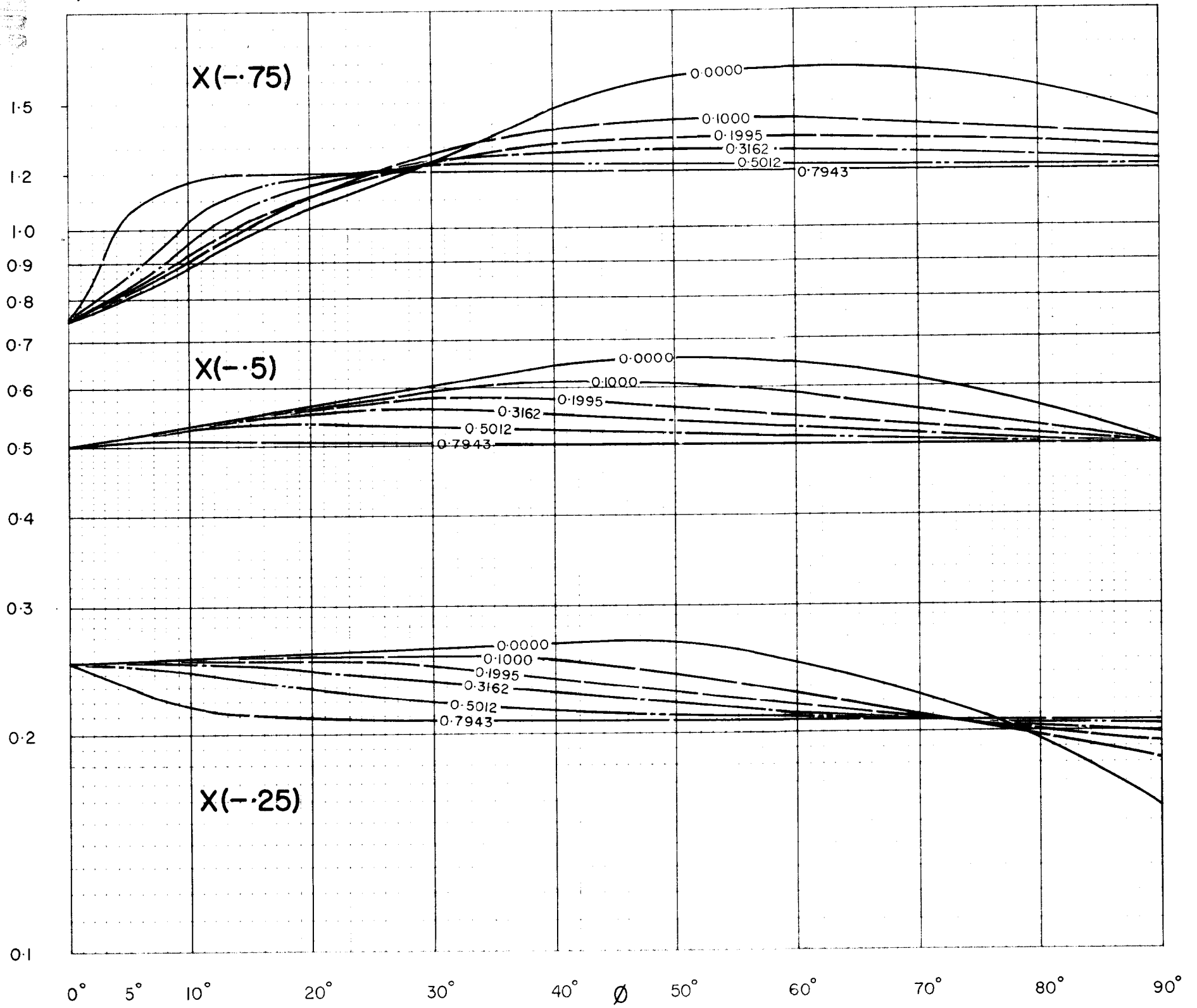
FIG. 3

5° 10° 15°

GRAVITY ANOMALY OF A
SLOPING CONTACT

DEPTH TO LOWER SURFACE = 1·0
DEPTH TO UPPER SURFACE INDICATED ON CURVES.
EXTENT OF SLOPE INDICATED BY THICKENED CURVE =
MIDPOINT OF SLOPE =
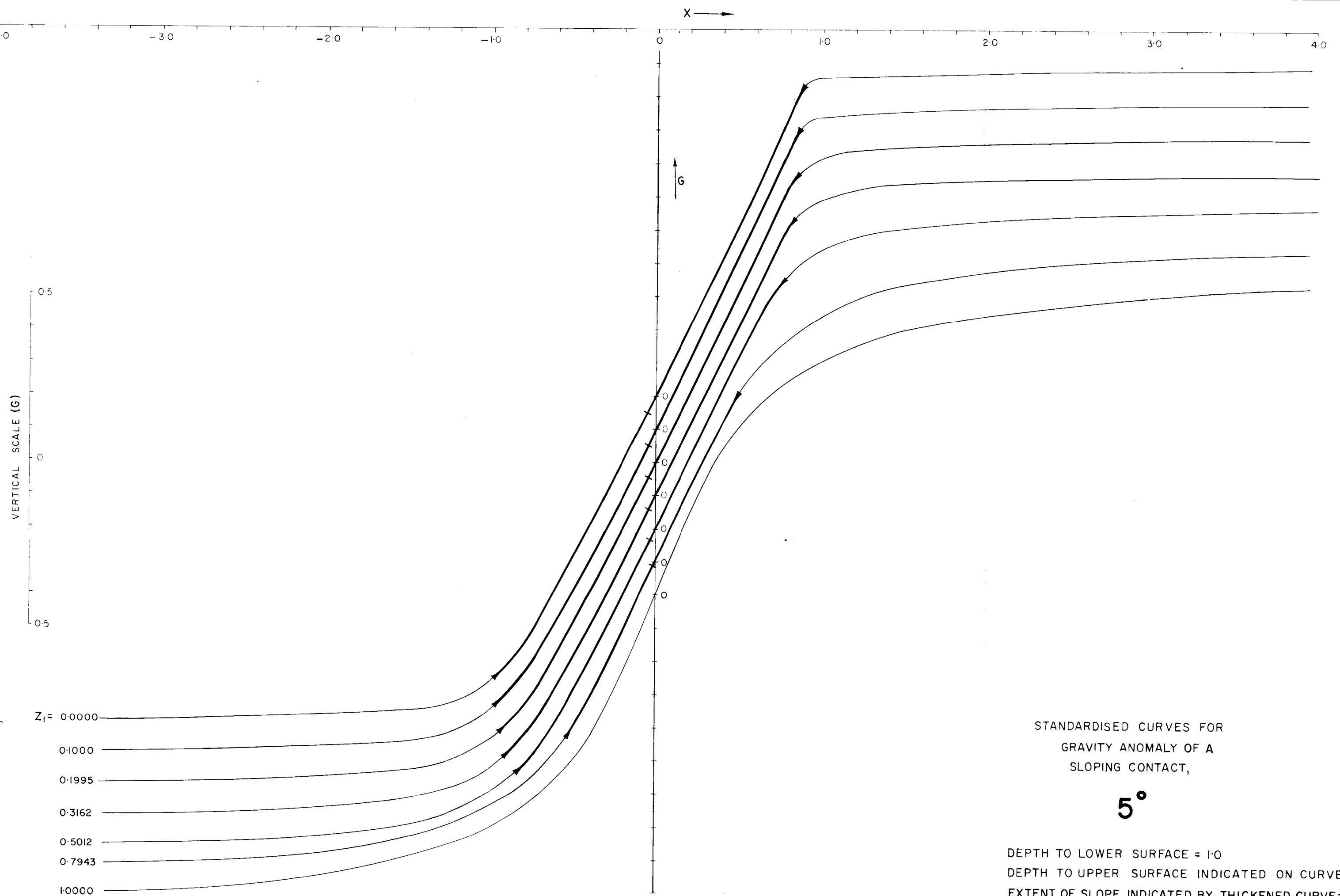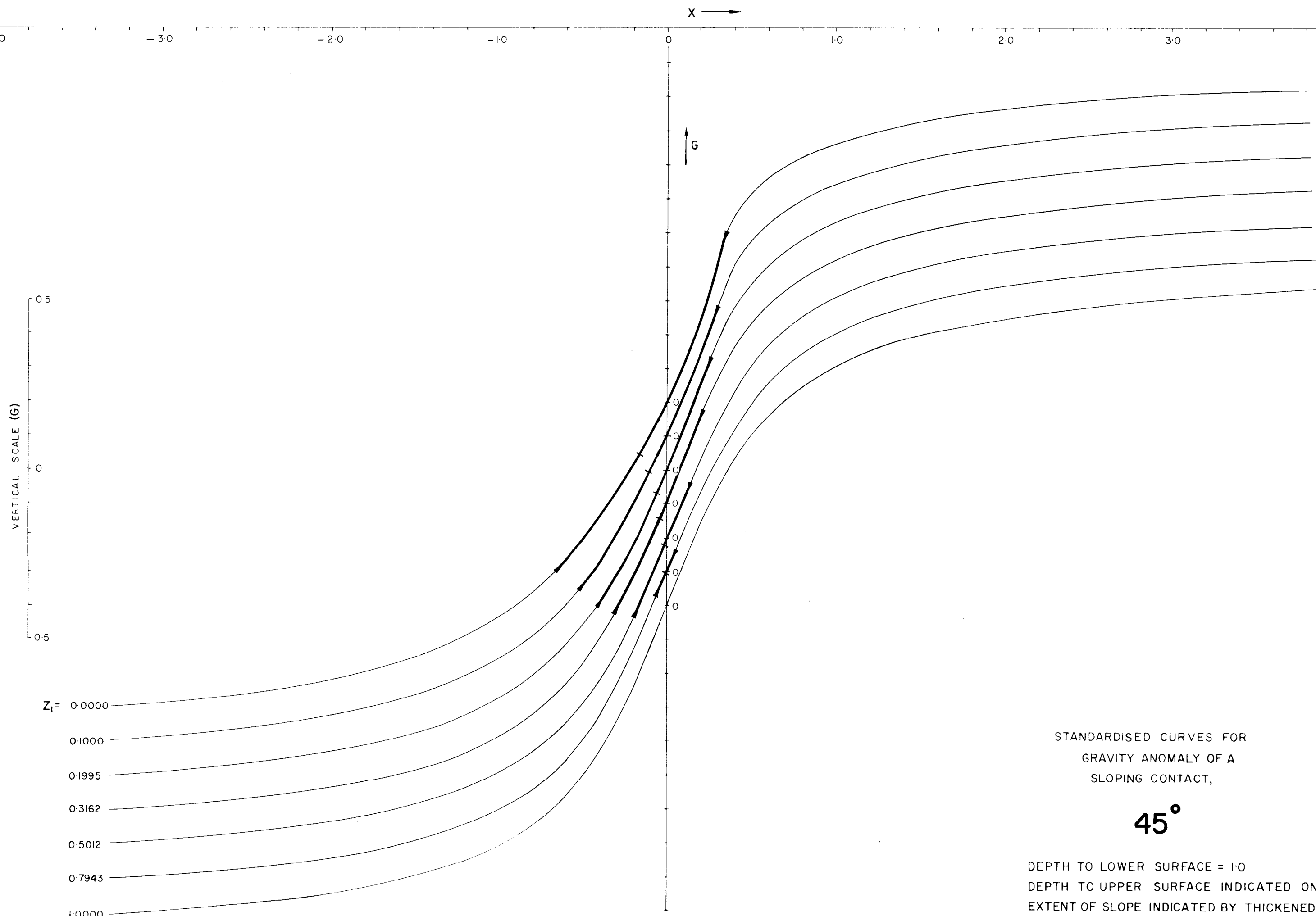
FIG. 4
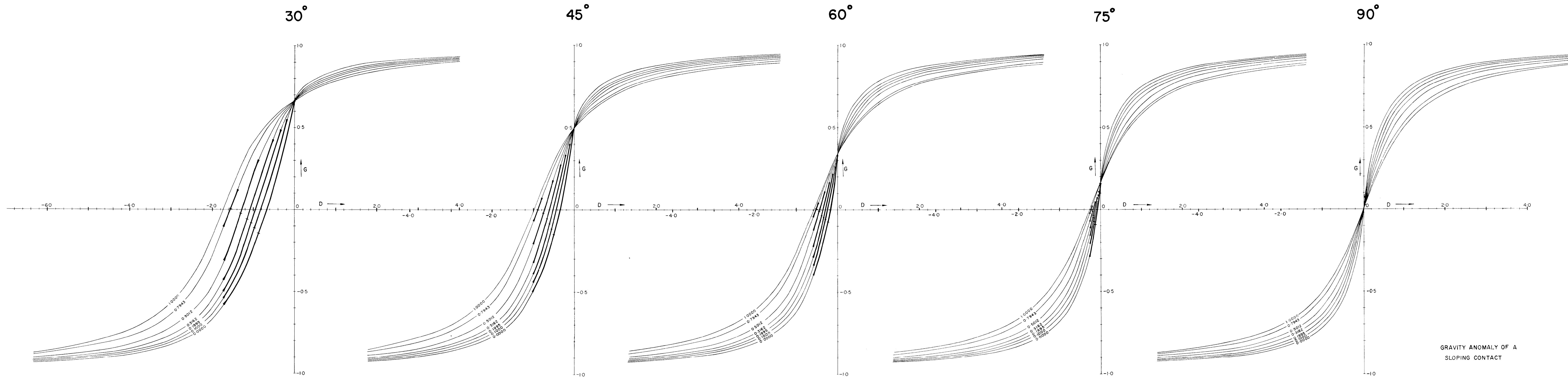
GRAVITY ANOMALY OF A
SLOPING CONTACT
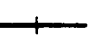
DEPTH TO LOWER SURFACE = 1·0
DEPTH TO UPPER SURFACE INDICATED ON CURVES.
EXTENT OF SLOPE INDICATED BY THICKENED CURVE = ▬▬▬
MIDPOINT OF SLOPE = ━┿━
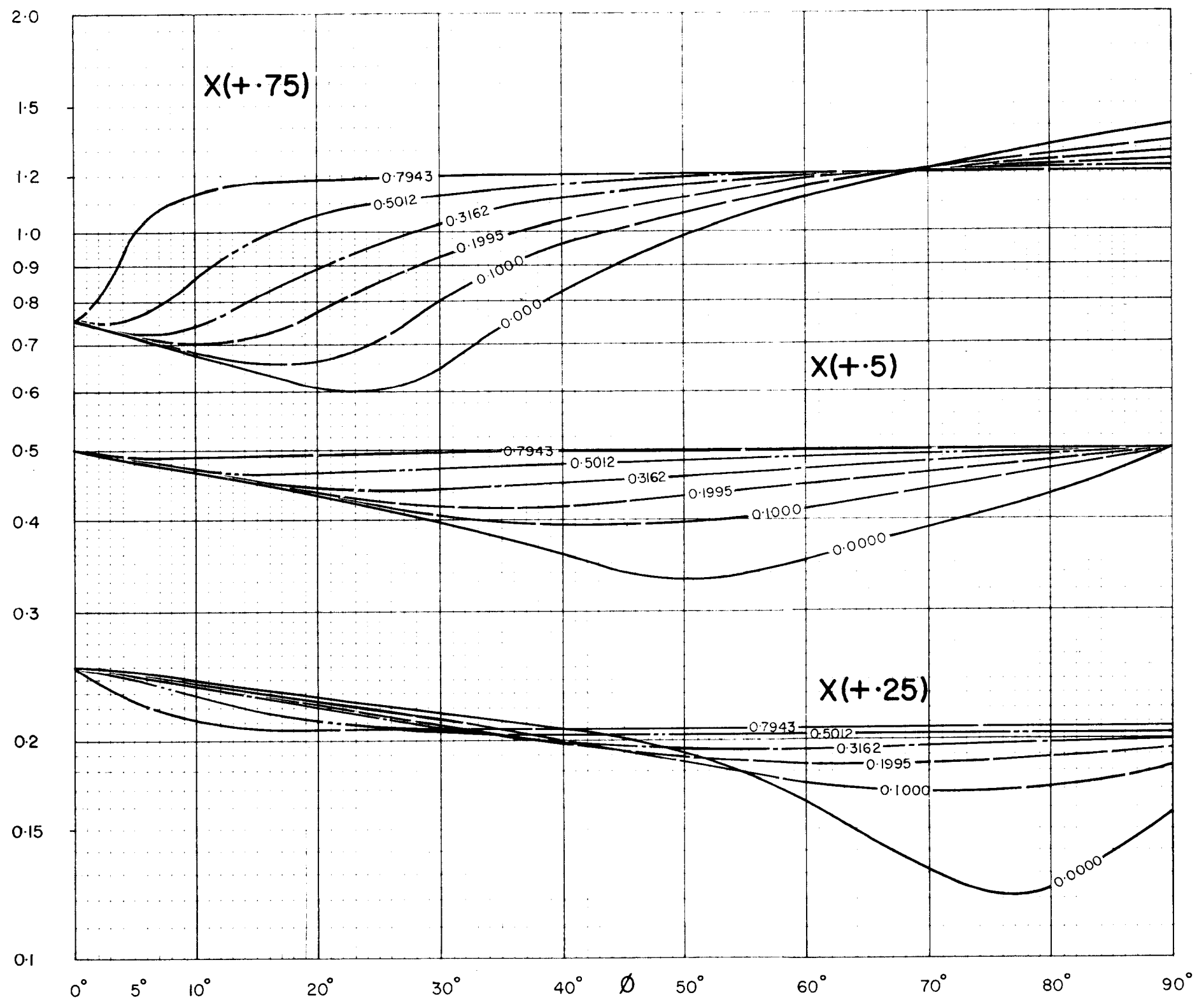
GRAVITY ANOMALY OF A SLOPING CONTACT
X PARAMETERS

FIG. 5

FIG. 6

STANDARDISED CURVES FOR
GRAVITY ANOMALY OF A
SLOPING CONTACT,

5°

DEPTH TO LOWER SURFACE = 1·0
DEPTH TO UPPER SURFACE INDICATED ON CURVES.
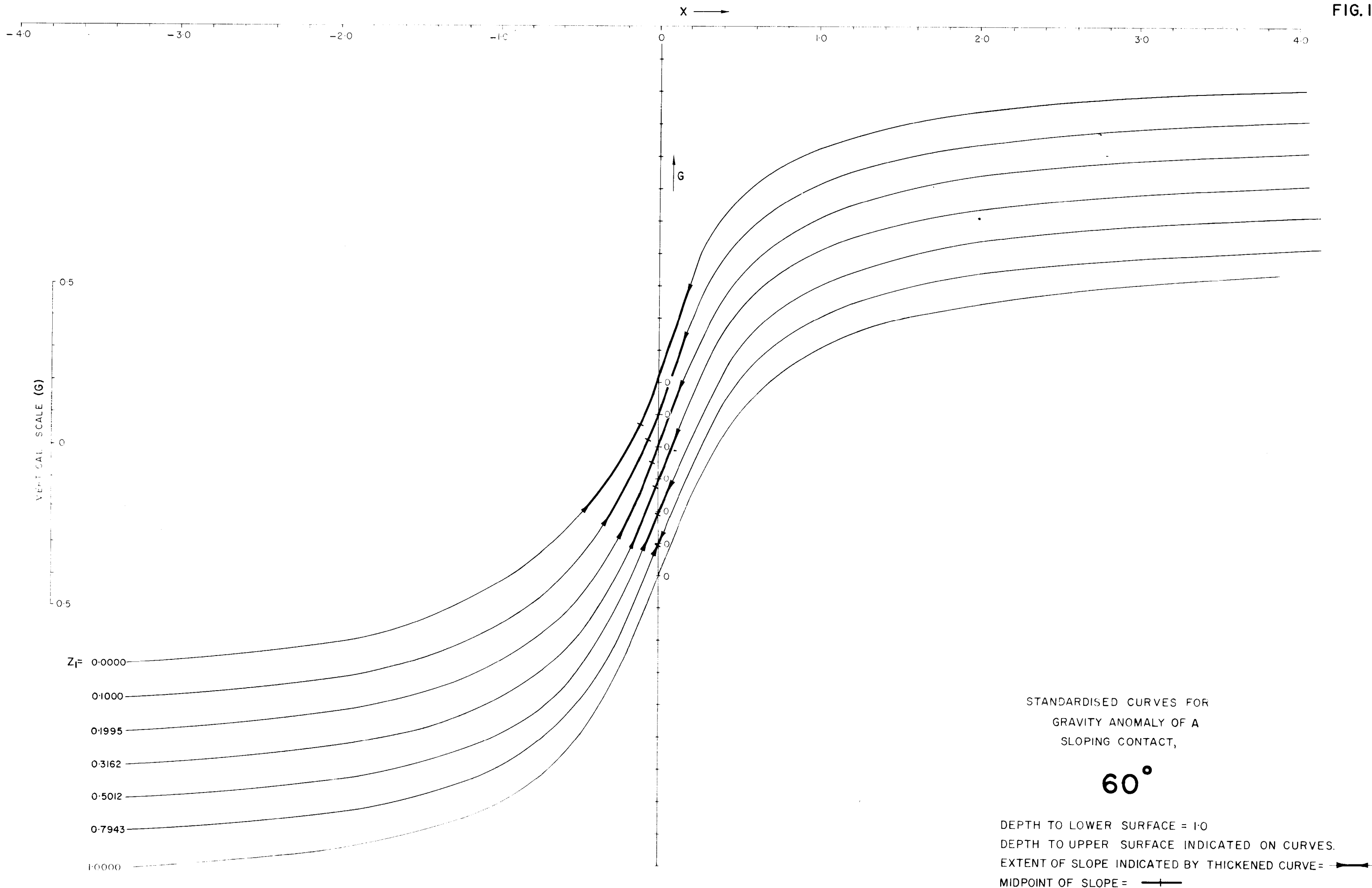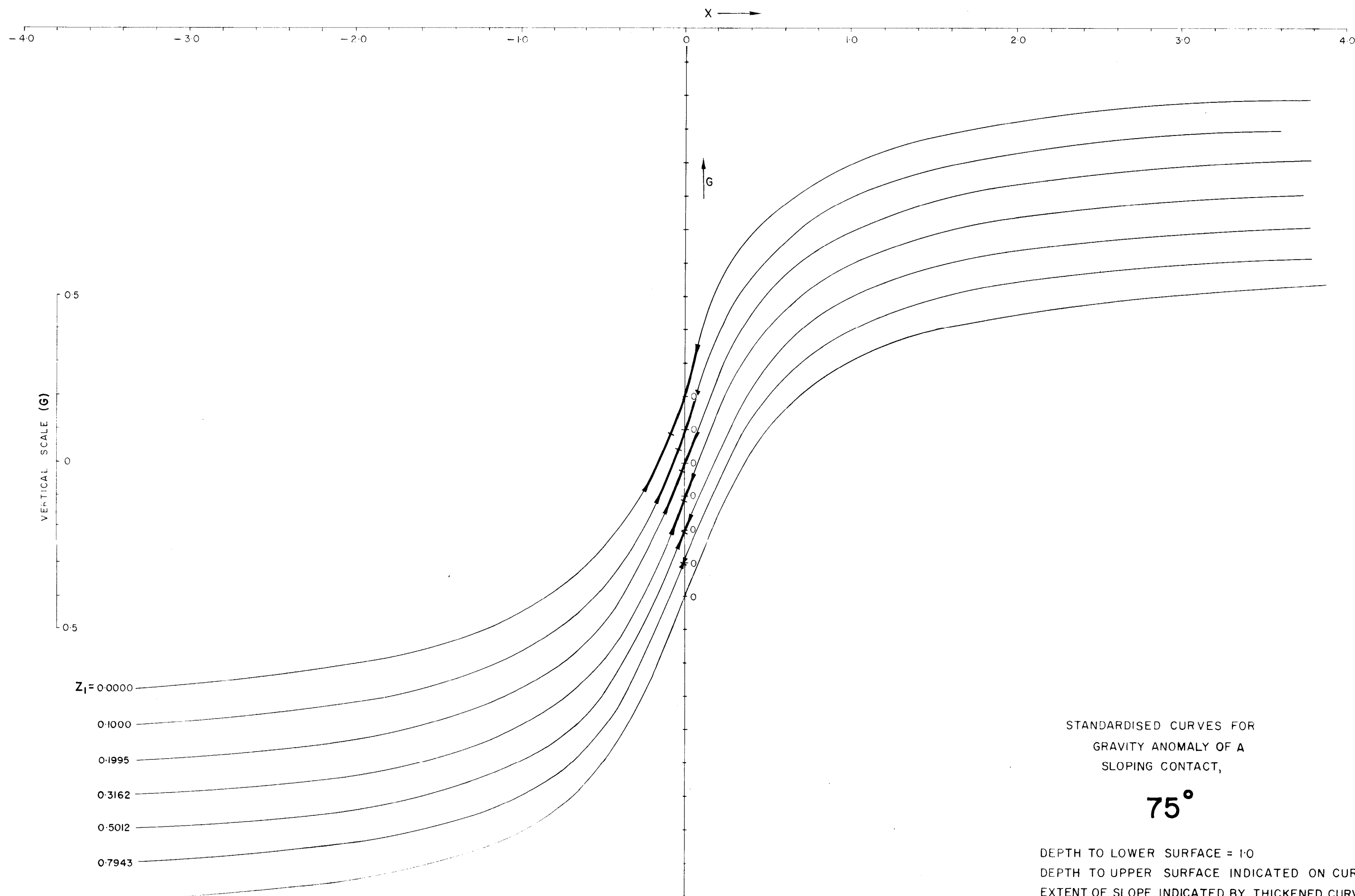EXTENT OF SLOPE INDICATED BY THICKENED CURVE=
MIDPOINT OF SLOPE =

Z_1= 0·0000
0·1000
0·1995
0·3162
0·5012
0·7943
1·0000

VERTICAL SCALE (G)

FIG. 7

STANDARDISED CURVES FOR
GRAVITY ANOMALY OF A
SLOPING CONTACT,

10°

DEPTH TO LOWER SURFACE = 1·0
DEPTH TO UPPER SURFACE INDICATED ON CURVES.
EXTENT OF SLOPE INDICATED BY THICKENED CURVE =
MIDPOINT OF SLOPE =

FIG. 8

X →

G

VERTICAL SCALE (G)

0·5

0

0·5

Z_1 = 0·0000

0·1000

0·1995

0·3162

0·5012

0·7943

1·0000

STANDARDISED CURVES FOR
GRAVITY ANOMALY OF A
SLOPING CONTACT,

15°

DEPTH TO LOWER SURFACE = 1·0
DEPTH TO UPPER SURFACE INDICATED ON CURVES.
EXTENT OF SLOPE INDICATED BY THICKENED CURVE =
MIDPOINT OF SLOPE = ┼

FIG. 9

STANDARDISED CURVES FOR
GRAVITY ANOMALY OF A
SLOPING CONTACT,

30°

DEPTH TO LOWER SURFACE = 1·0
DEPTH TO UPPER SURFACE INDICATED ON CURVES.
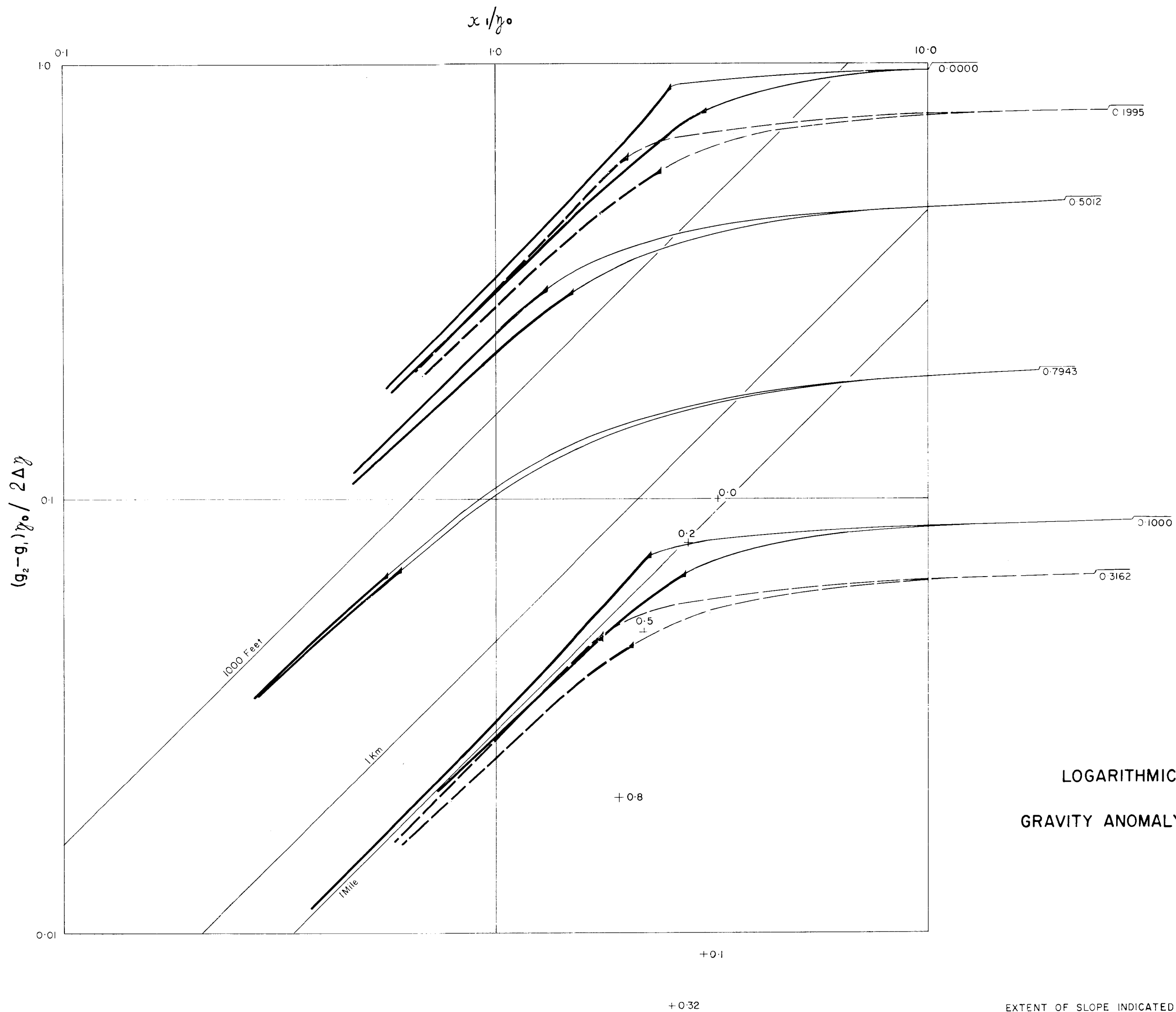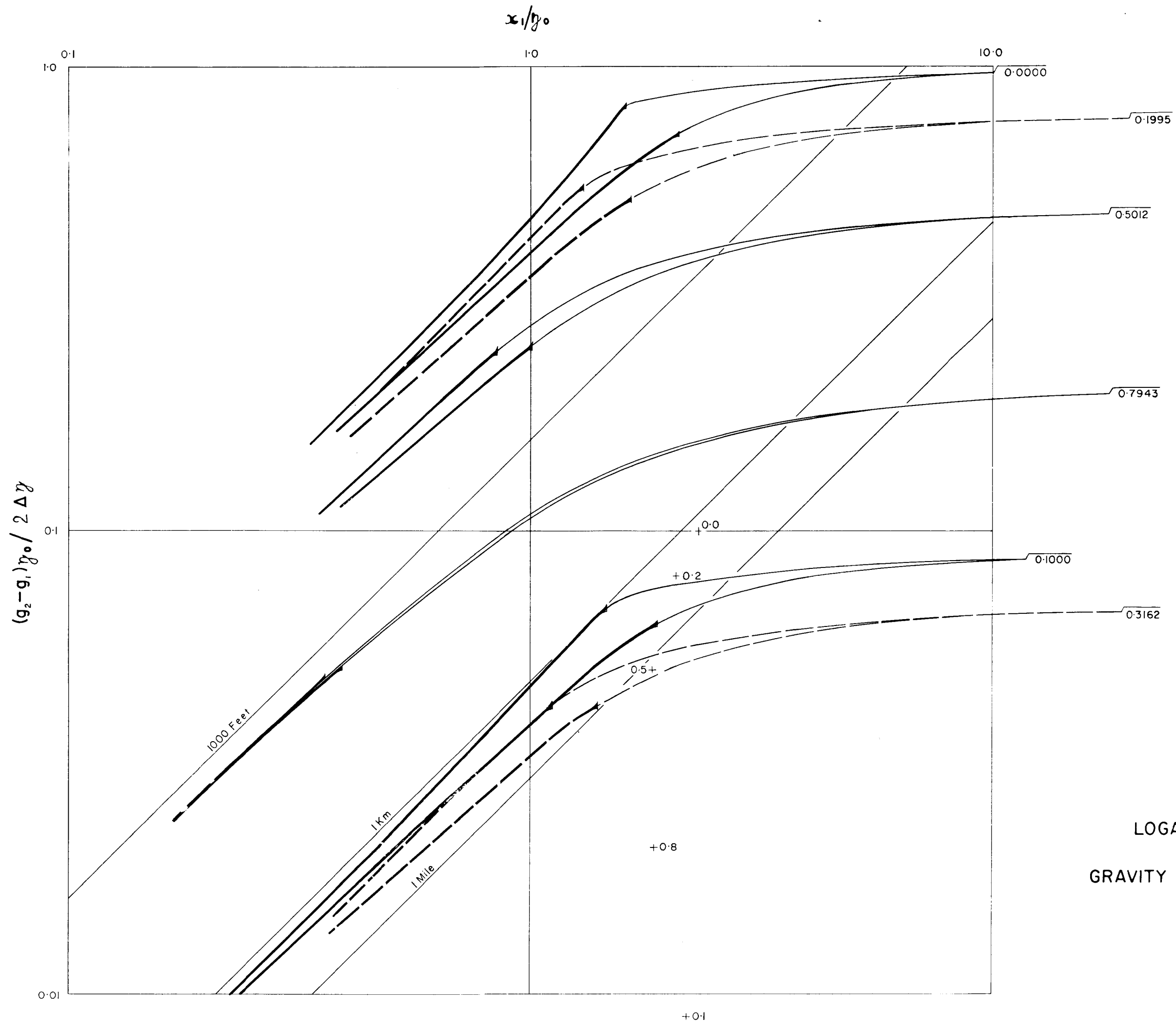EXTENT OF SLOPE INDICATED BY THICKENED CURVE = ➤
MIDPOINT OF SLOPE = ┼

$Z_1 =$ 0·0000
0·1000
0·1995
0·3162
0·5012
0·7943
1·0000

FIG. 10

STANDARDISED CURVES FOR
GRAVITY ANOMALY OF A
SLOPING CONTACT,

45°

DEPTH TO LOWER SURFACE = 1·0
DEPTH TO UPPER SURFACE INDICATED ON CURVES.
EXTENT OF SLOPE INDICATED BY THICKENED CURVE =
MIDPOINT OF SLOPE =

$Z_1 =$ 0·0000
0·1000
0·1995
0·3162
0·5012
0·7943
1·0000

VERTICAL SCALE (G)

FIG. 11

STANDARDISED CURVES FOR
GRAVITY ANOMALY OF A
SLOPING CONTACT,

60°

DEPTH TO LOWER SURFACE = 1·0
DEPTH TO UPPER SURFACE INDICATED ON CURVES.
EXTENT OF SLOPE INDICATED BY THICKENED CURVE = ➤
MIDPOINT OF SLOPE = ┼

FIG.12

STANDARDISED CURVES FOR
GRAVITY ANOMALY OF A
SLOPING CONTACT,

75°

DEPTH TO LOWER SURFACE = 1·0
DEPTH TO UPPER SURFACE INDICATED ON CURVES.
EXTENT OF SLOPE INDICATED BY THICKENED CURVE = ▶
MIDPOINT OF SLOPE = ┼

$Z_1 = 0.0000$

0·1000

0·1995

0·3162

0·5012

0·7943

1·0000

FIG. 13

STANDARDISED CURVES FOR
GRAVITY ANOMALY OF A
SLOPING CONTACT,

90°

DEPTH TO LOWER SURFACE = 1·0
DEPTH TO UPPER SURFACE INDICATED ON CURVES.
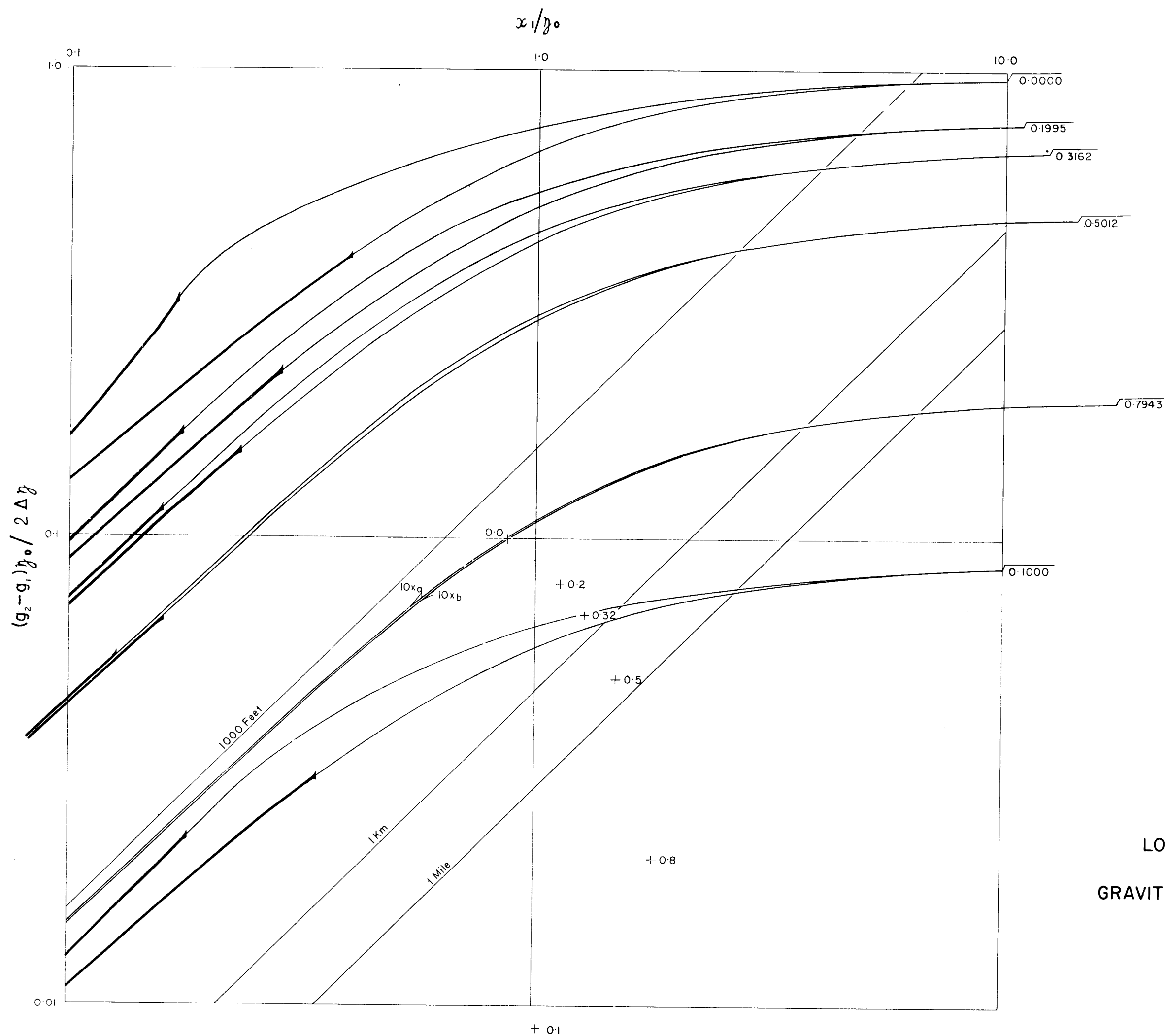EXTENT OF SLOPE INDICATED BY THICKENED CURVE =
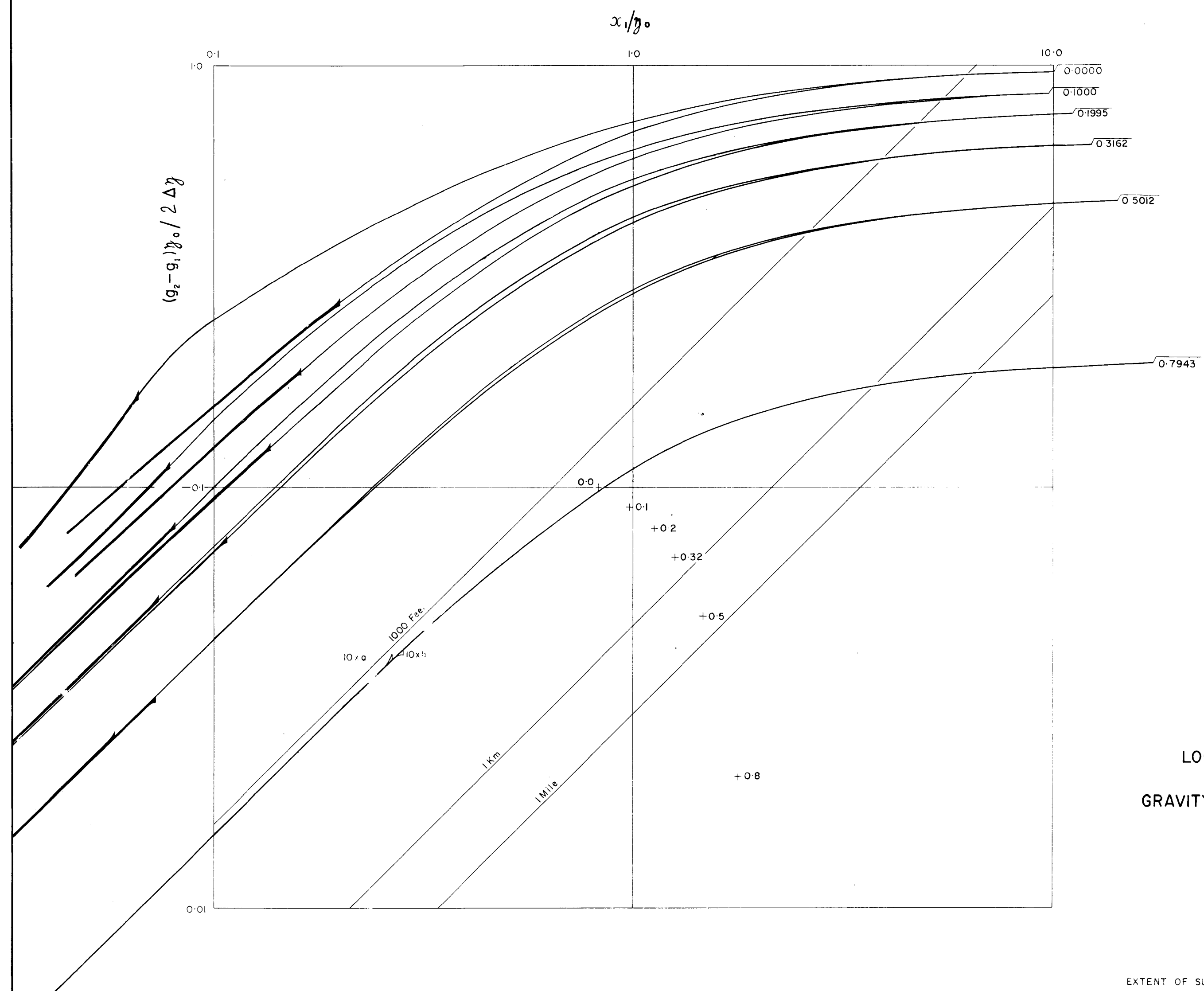MIDPOINT OF SLOPE =

FIG. 14
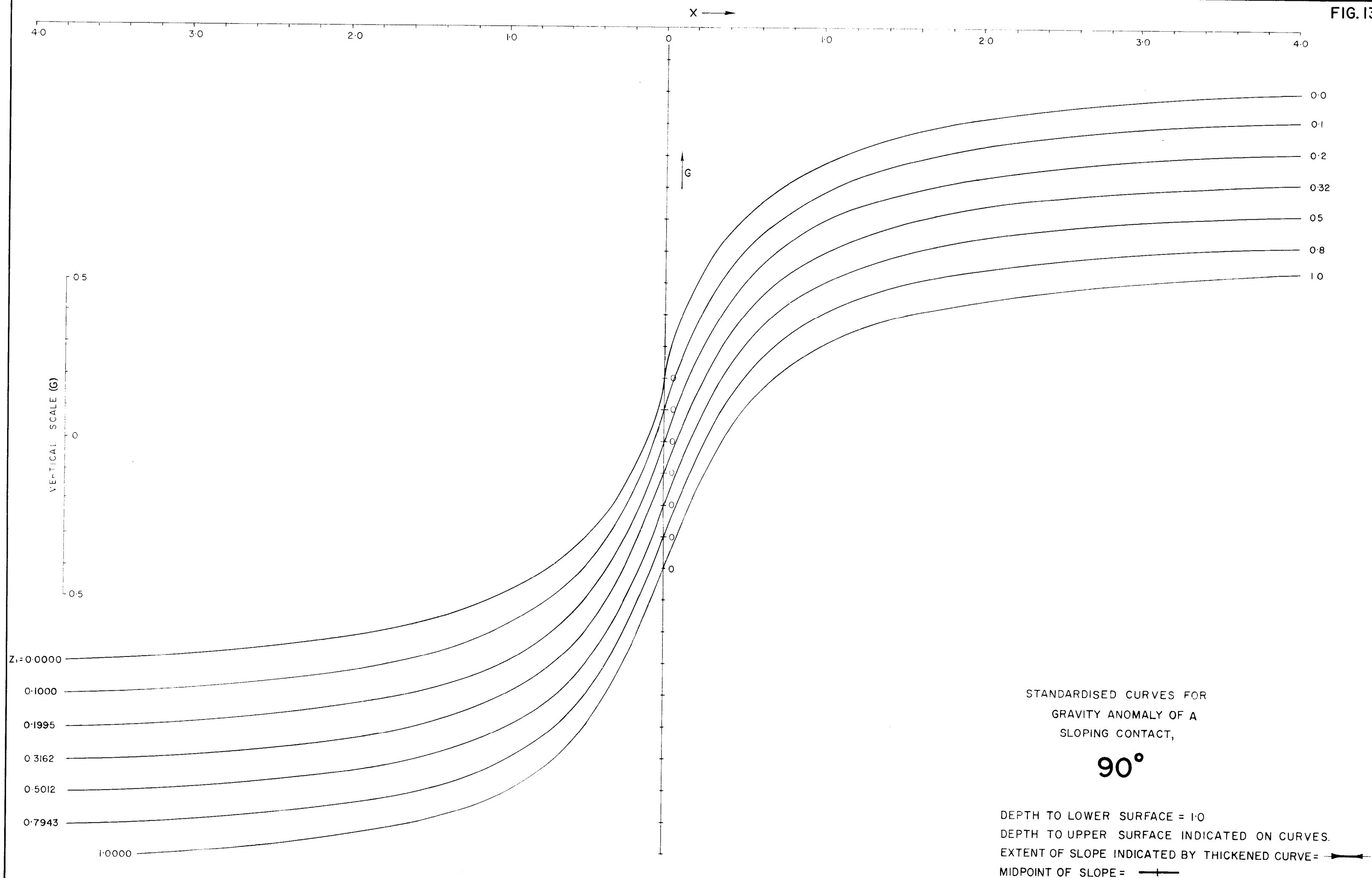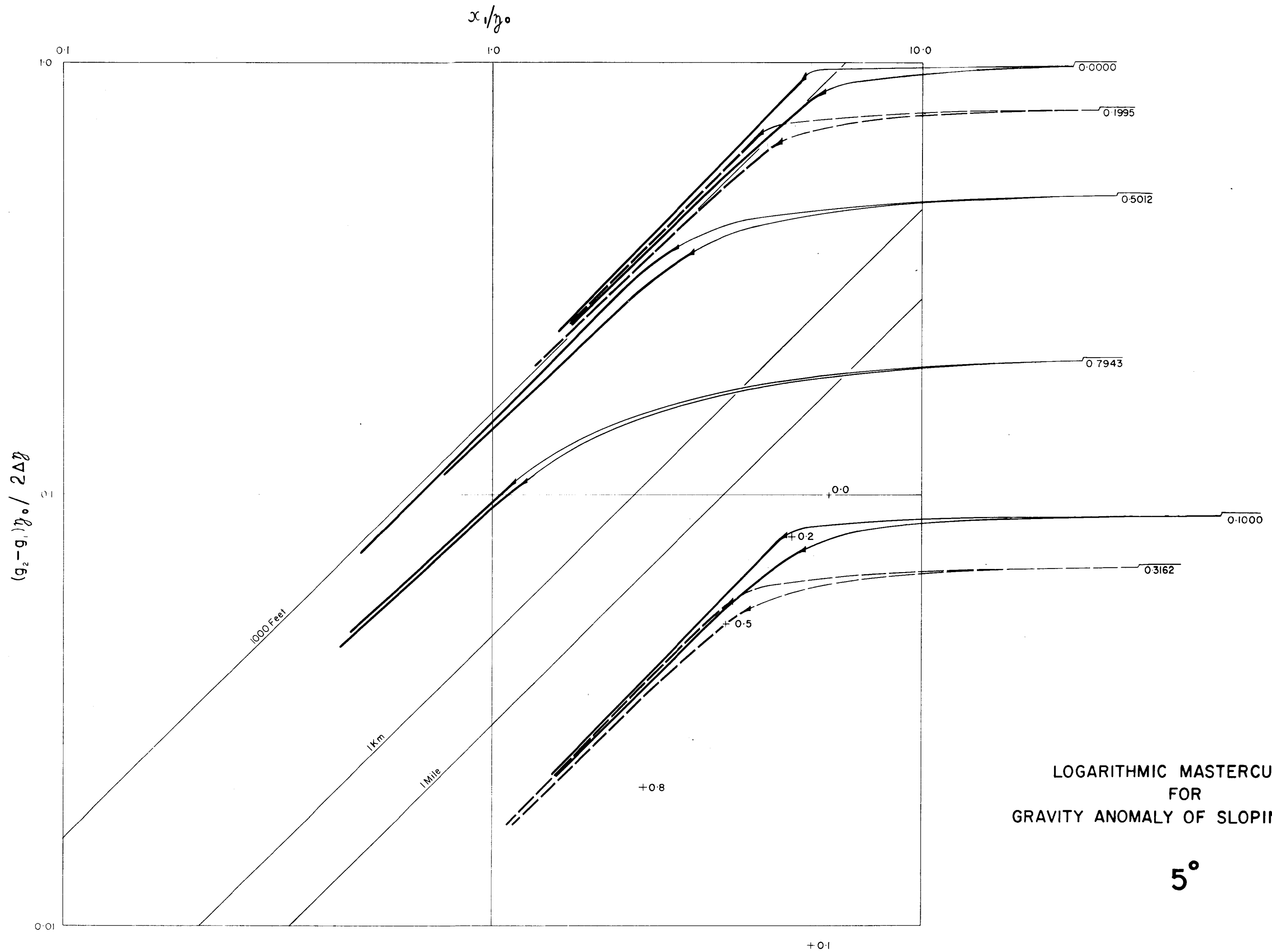
LOGARITHMIC MASTERCURVES
FOR
GRAVITY ANOMALY OF SLOPING FAULT

5°

EXTENT OF SLOPE INDICATED BY THICKENED CURVE

FIG. 15

x_1/y_0

$(g_2 - g_1) y_0 / 2\Delta y$

0.0000

0.1995

0.5012

0.7943

0.1000

0.3162

0.0

0.2

0.5

+ 0.8

1000 Feet

1 Km

1 Mile

LOGARITHMIC MASTERCURVES
FOR
GRAVITY ANOMALY OF SLOPING FAULT

10°

+ 0.32

+ 0.1

EXTENT OF SLOPE INDICATED BY THICKENED CURVE

Geophysical Branch, Bureau of Mineral Resources, Geology and Geophysics.   G69- 498

TO ACCOMPANY RECORD No.1966/86

FIG. 16

x_1/g_0

LOGARITHMIC MASTERCURVES
FOR
GRAVITY ANOMALY OF SLOPING FAULT

15°

EXTENT OF SLOPE INDICATED BY THICKENED CURVE

Geophysical Branch, Bureau of Mineral Resources, Geology and Geophysics.

G69-499

TO ACCOMPANY RECORD No. 1966/86

FIG. 17

x_1/y_0

LOGARITHMIC MASTERCURVES
FOR
GRAVITY ANOMALY OF SLOPING FAULT

30°

EXTENT OF SLOPE INDICATED BY THICKENED CURVE

FIG. 18

x_1/z_0
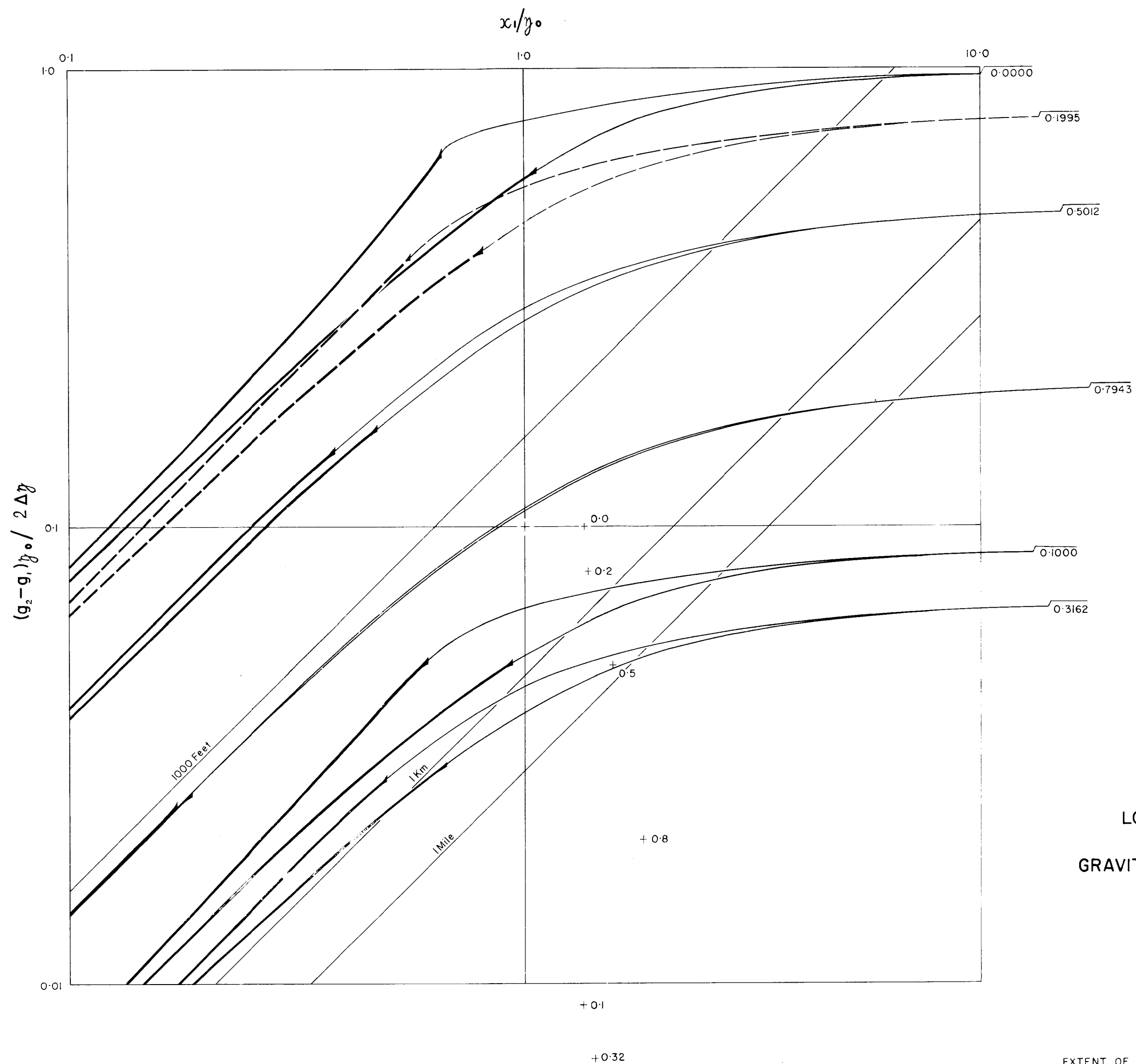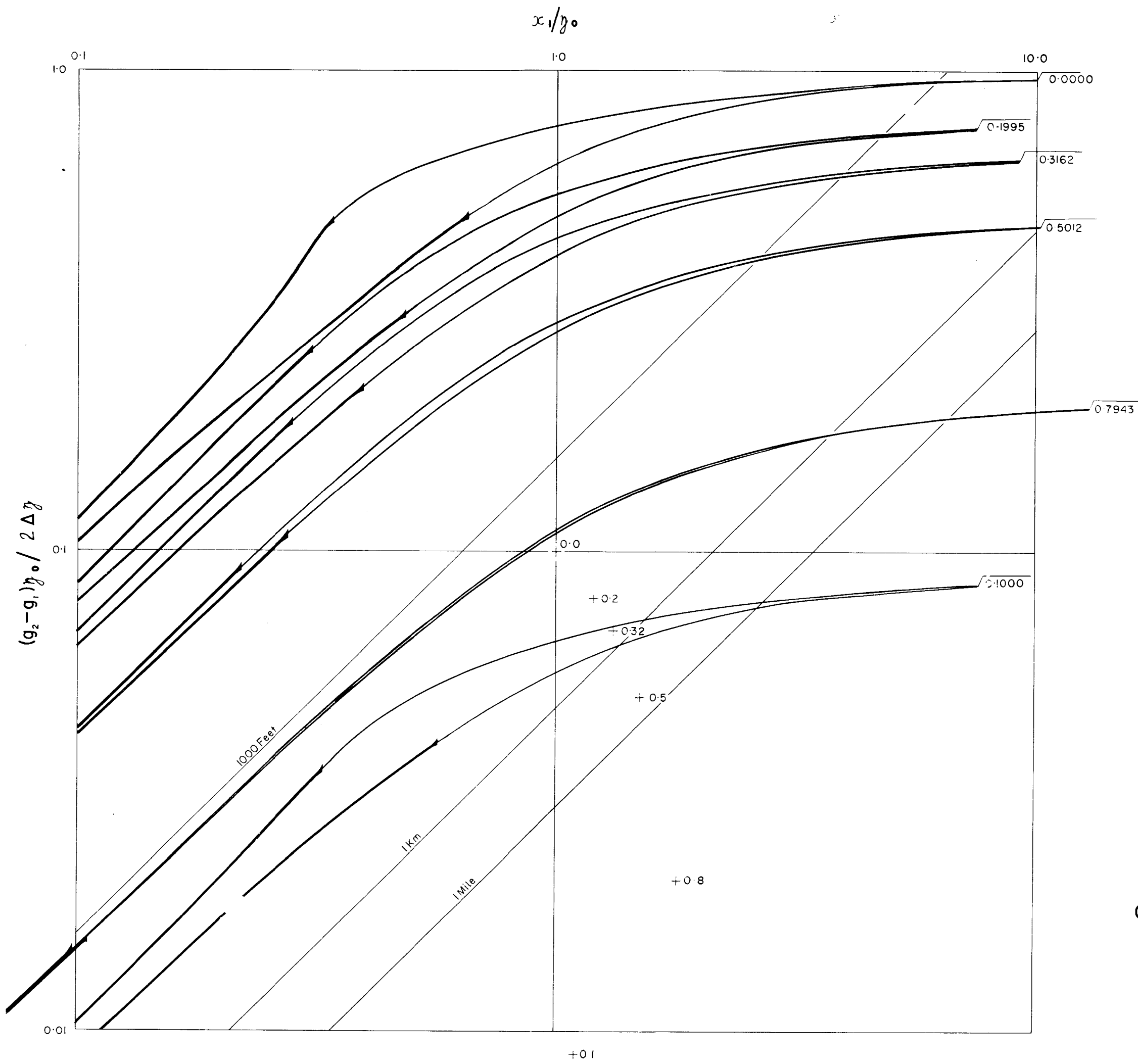
LOGARITHMIC MASTERCURVES
FOR
GRAVITY ANOMALY OF SLOPING FAULT

45°

EXTENT OF SLOPE INDICATED BY THICKENED CURVE
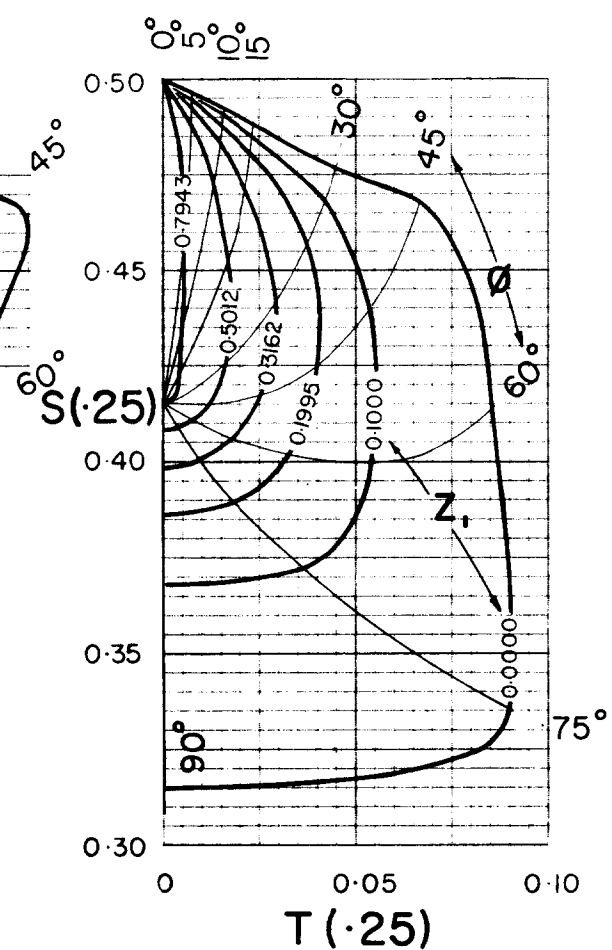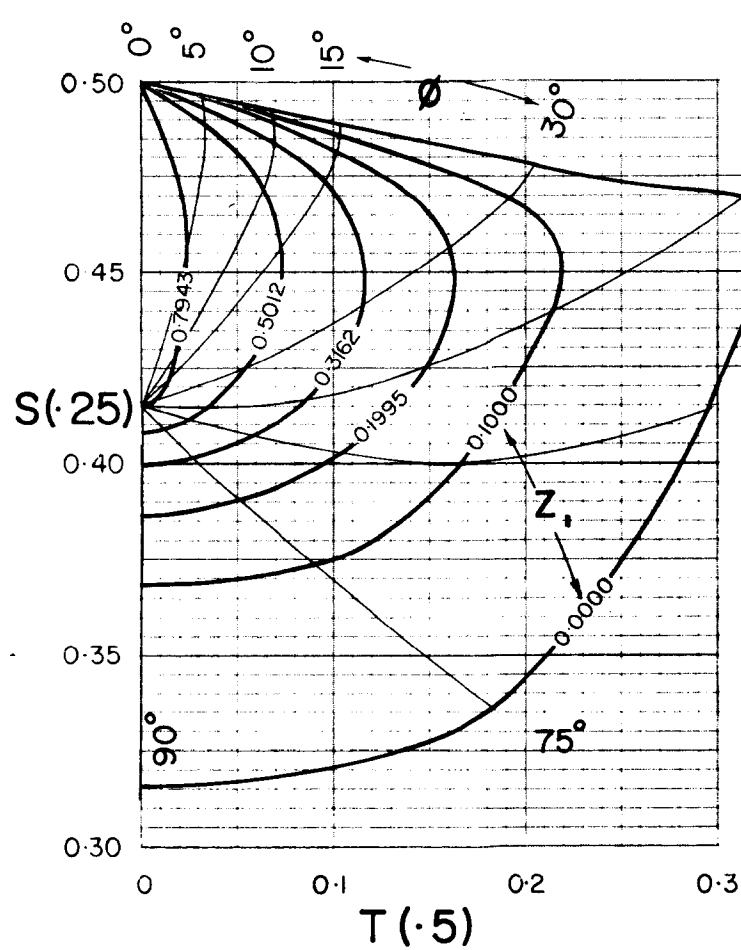
FIG.19

x_1/z_0

$(g_2-g_1)z_0 / 2\Delta\gamma$

LOGARITHMIC MASTERCURVES
FOR
GRAVITY ANOMALY OF SLOPING FAULT

60°

EXTENT OF SLOPE INDICATED BY THICKENED CURVE

Geophysical Branch, Bureau of Mineral Resources, Geology and Geophysics.

G69-502

TO ACCOMPANY RECORD No.1966/86

FIG. 20

$x_1/\mathfrak{z}_0$

$(g_2 - g_1)\mathfrak{z}_0 / 2\,\Delta\mathfrak{z}$

0·0000
0·1000
0·1995
0·3162
0·5012
0·7943

0·0
+0·1
+0·2
+0·32
+0·5
+0·8

1000 Feet
10 × a
10 × b
1 Km
1 Mile

LOGARITHMIC MASTERCURVES
FOR
GRAVITY ANOMALY OF SLOPING FAULT

75°

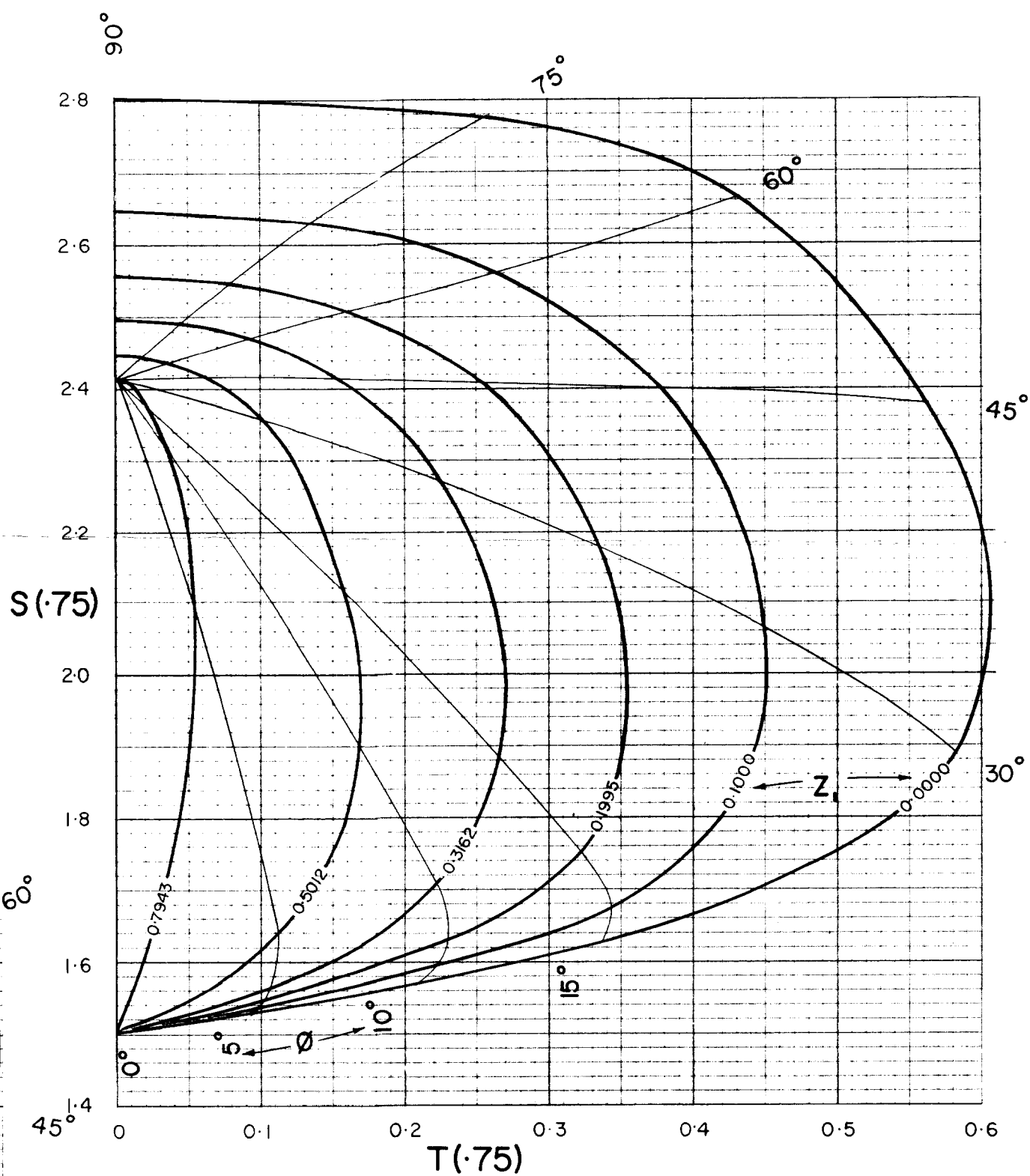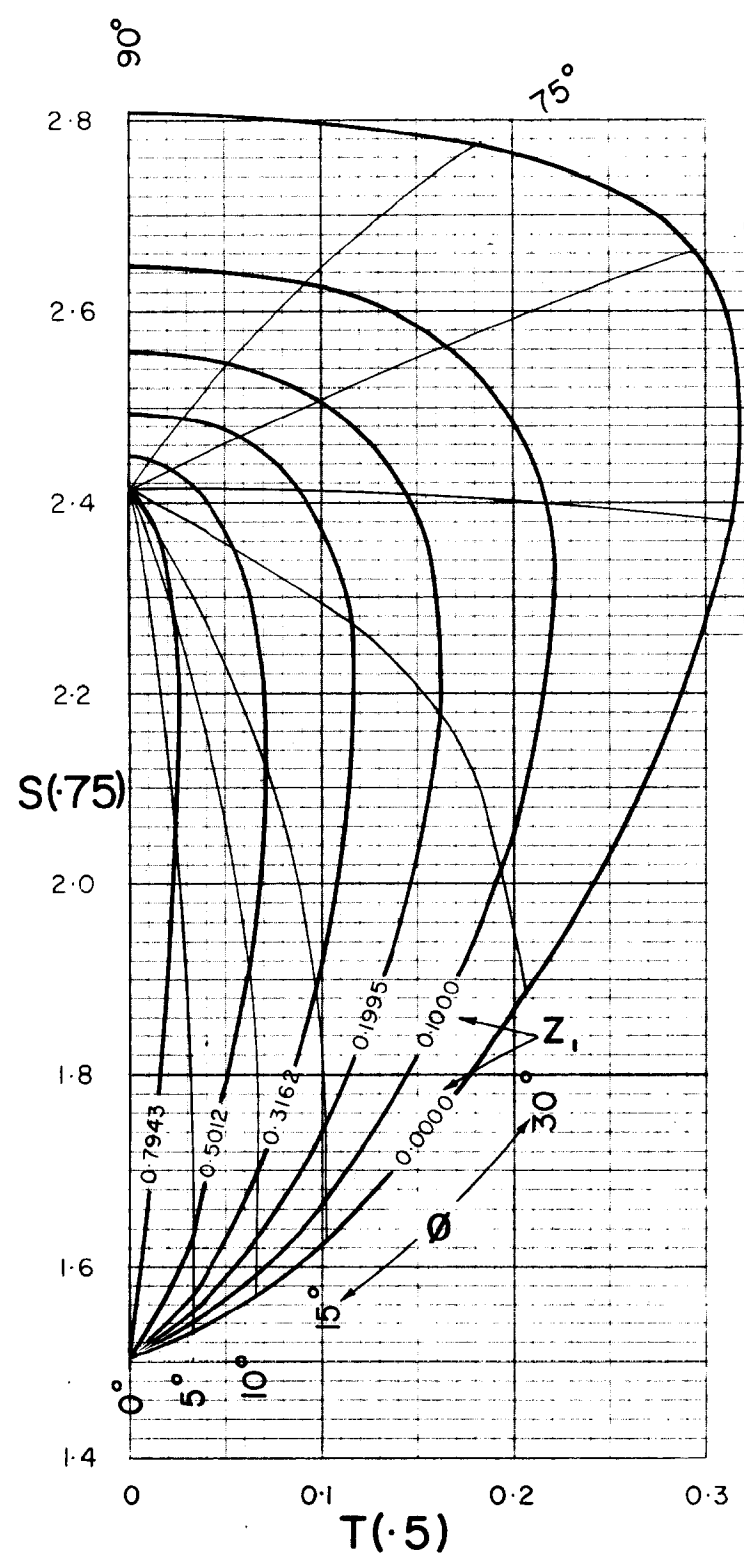EXTENT OF SLOPE INDICATED BY THICKENED CURVE

FIG. 21
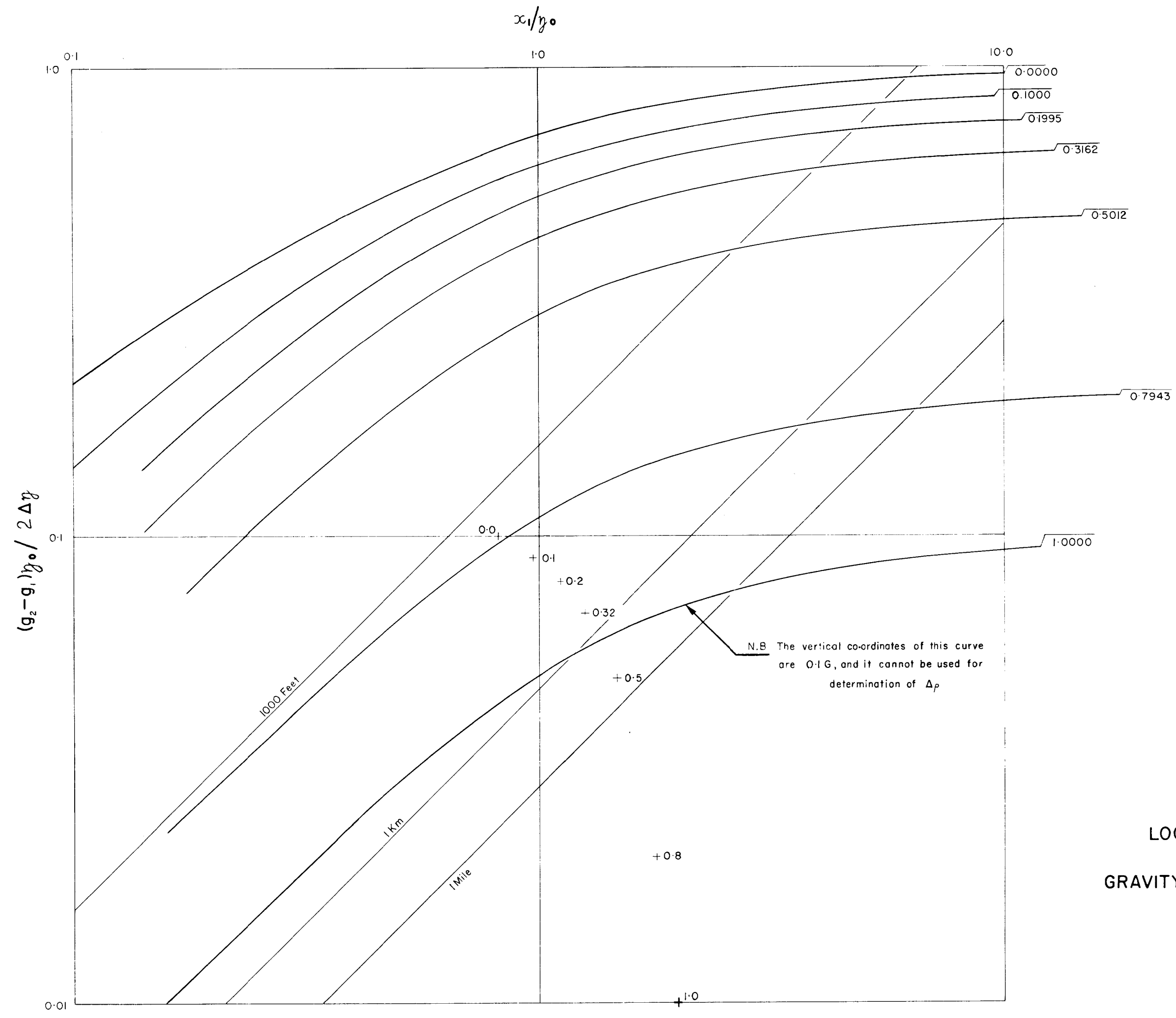
LOGARITHMIC MASTERCURVES
FOR
GRAVITY ANOMALY OF SLOPING FAULT

90°

FIG. 22
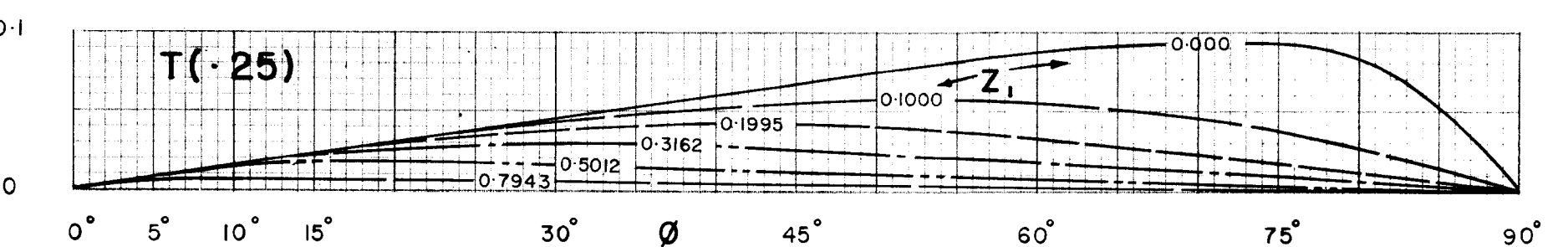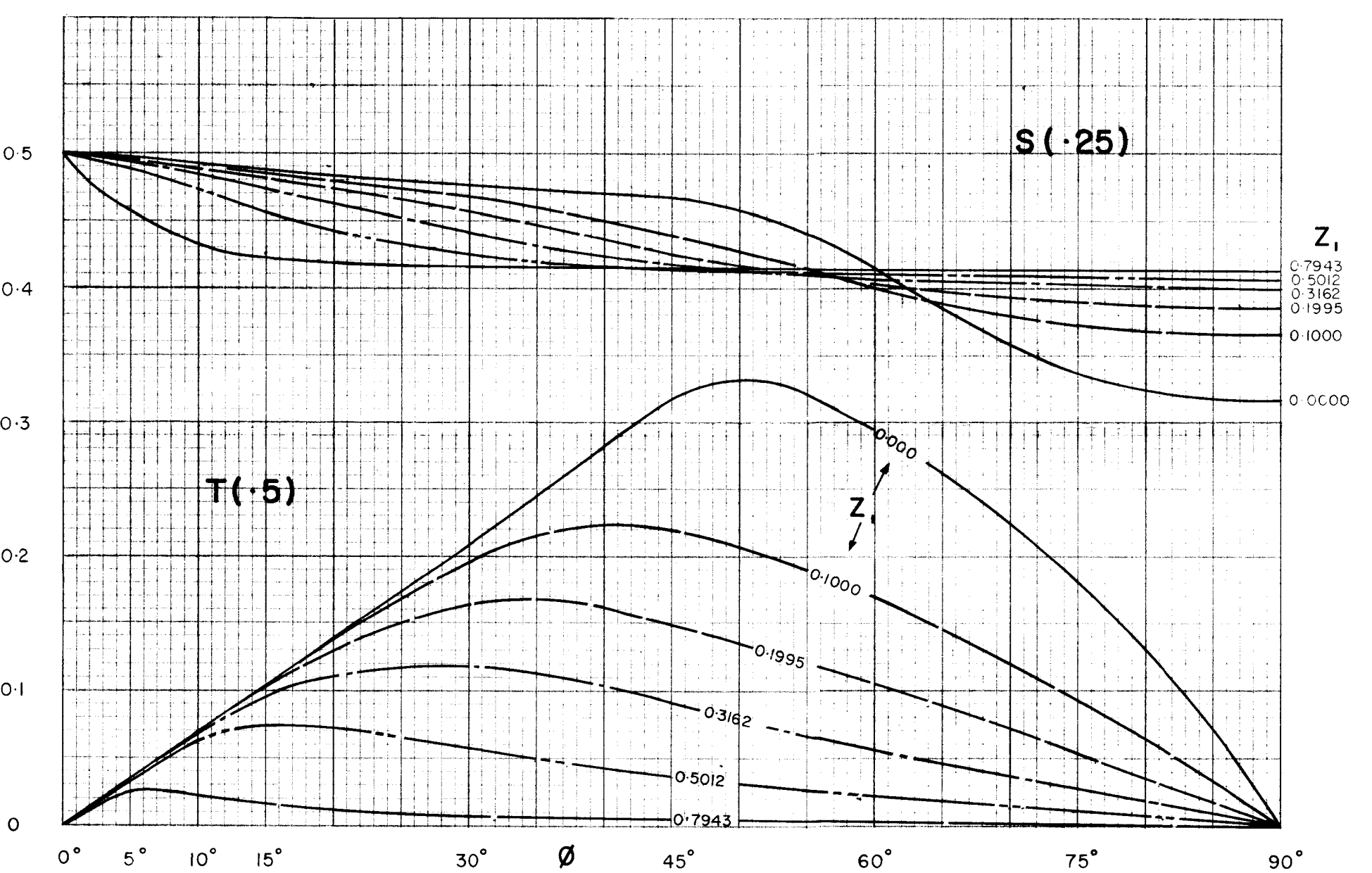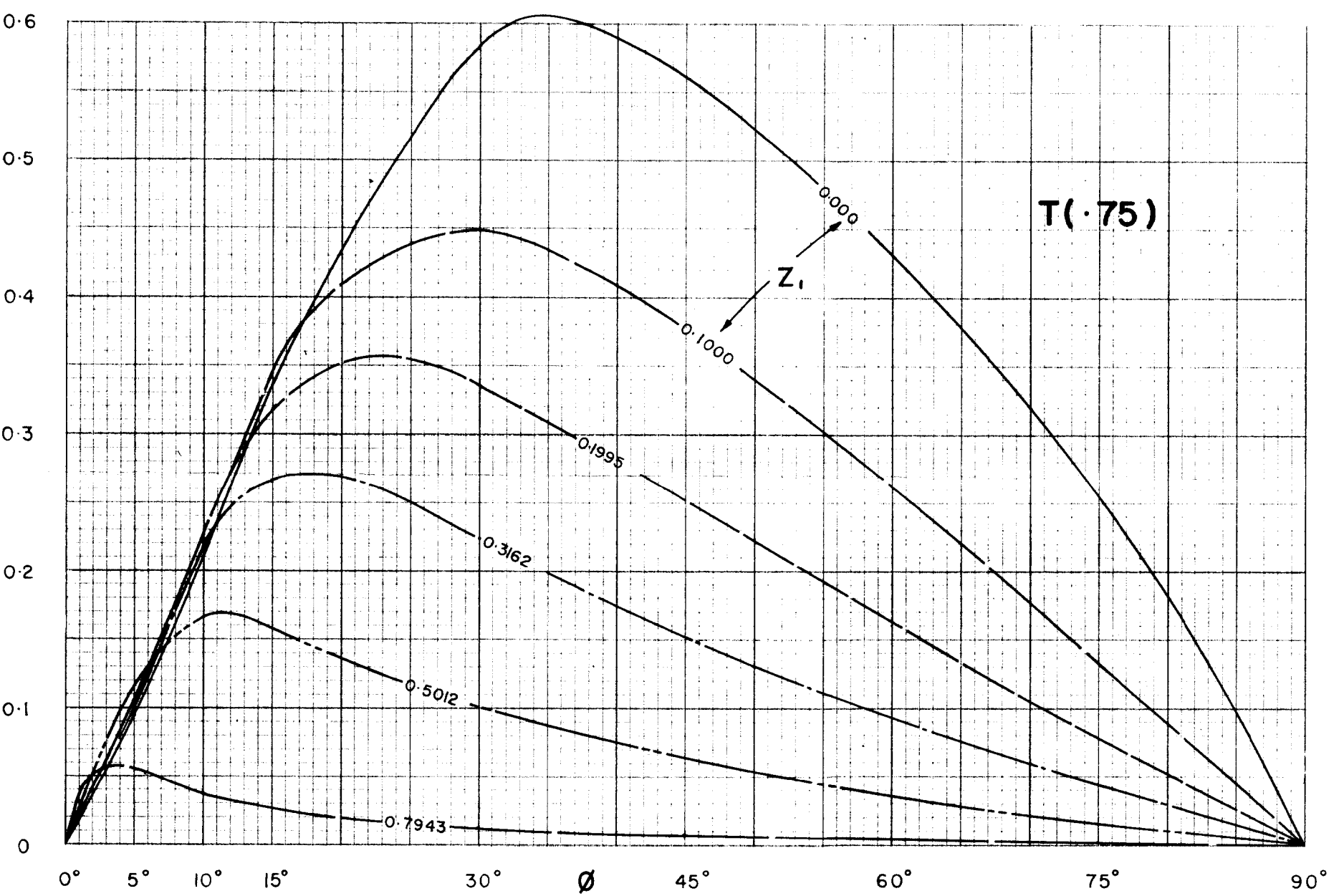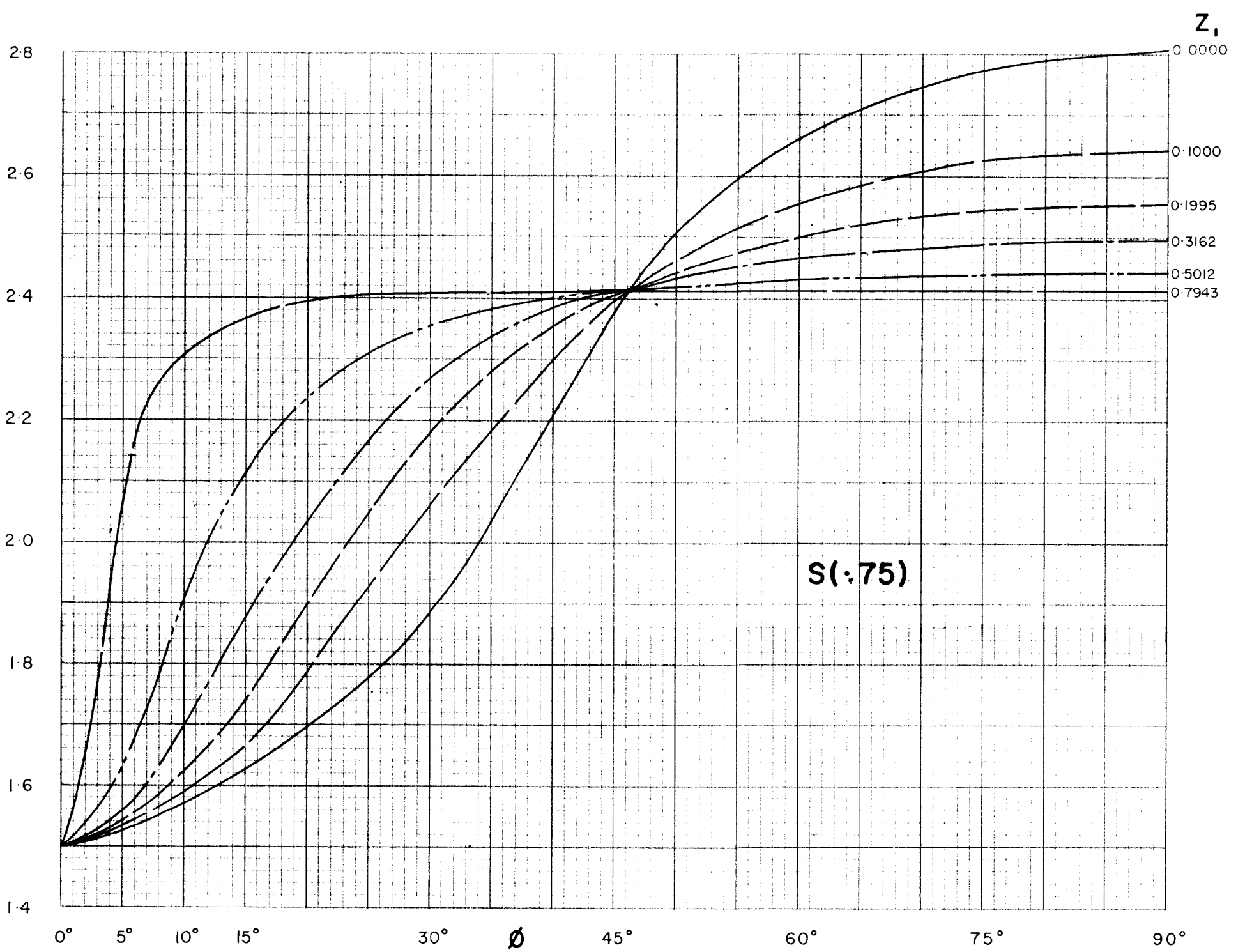
GRAVITY ANOMALY OF A SLOPING CONTACT
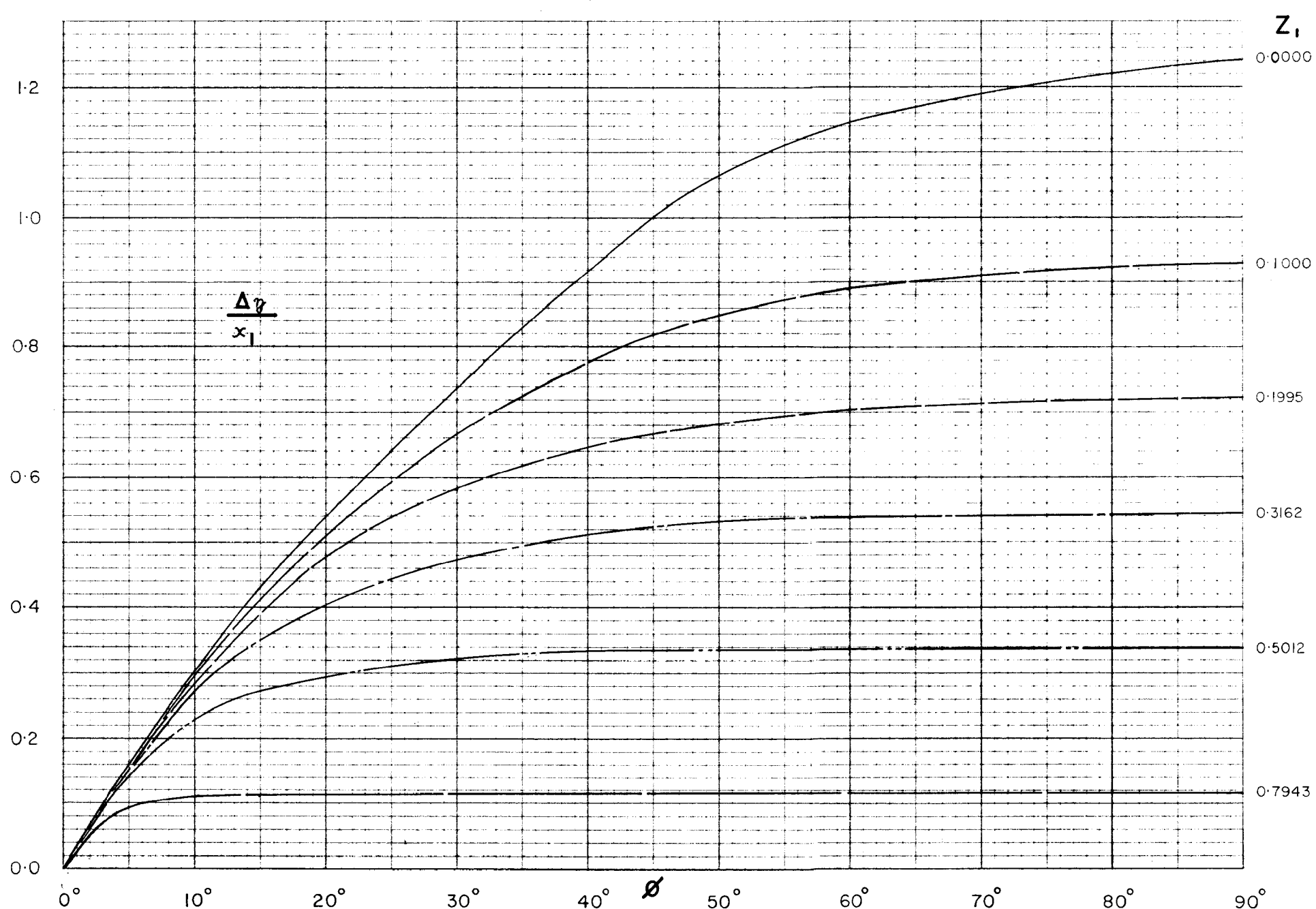PARAMETERS S AND T

G69—489

TO ACCOMPANY RECORD No.1966/86

FIG.23

FIGURE 23
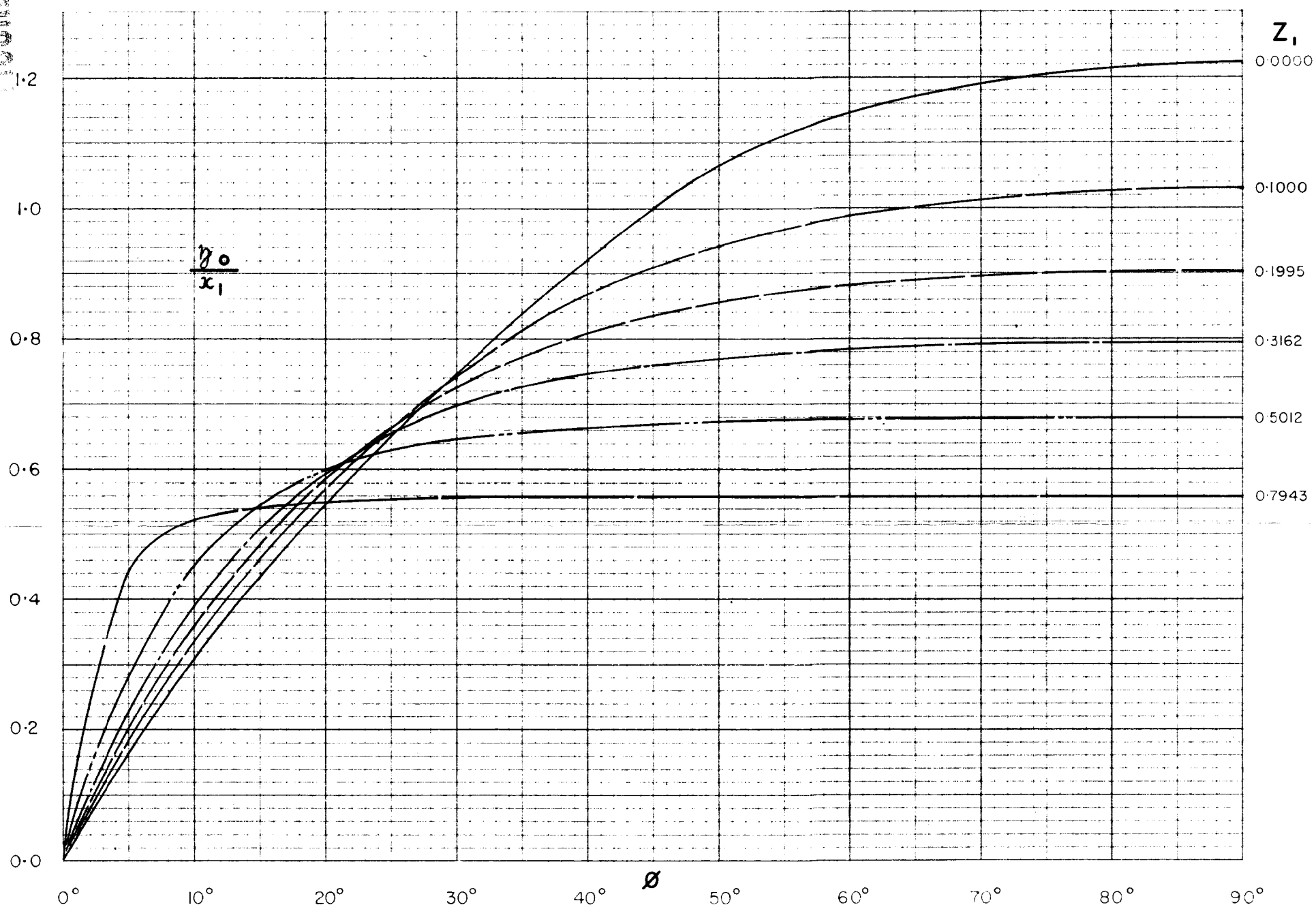
GRAVITY ANOMALY OF A SLOPING
CONTACT

CHARTS FOR IDENTIFICATION OF
SLOPE AND DEPTH FROM S AND T
PARAMETERS

Geophysical Branch, Bureau of Mineral Resources, Geology and Geophysics

G69—491

TO ACCOMPANY RECORD No.1966/86

FIG.24
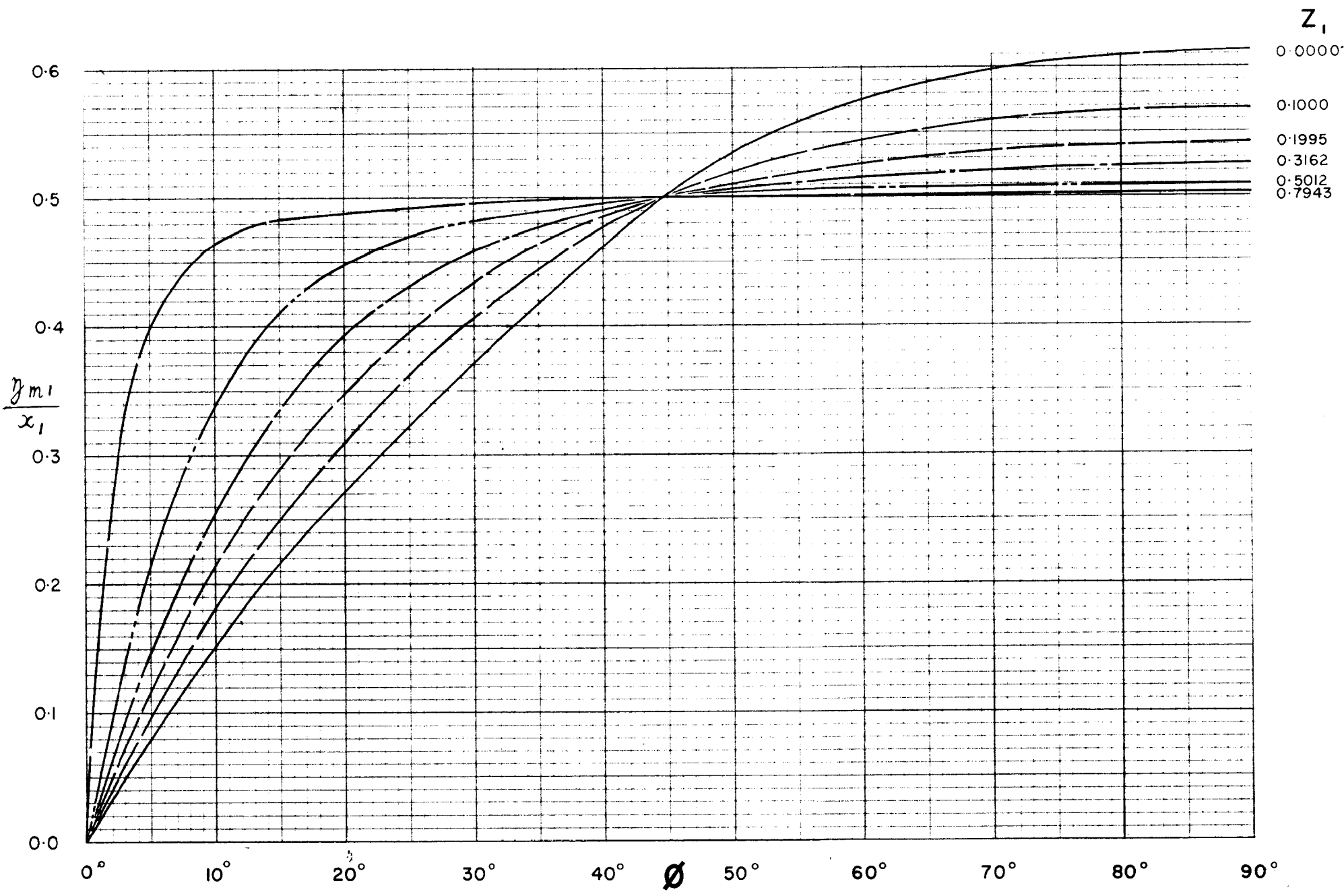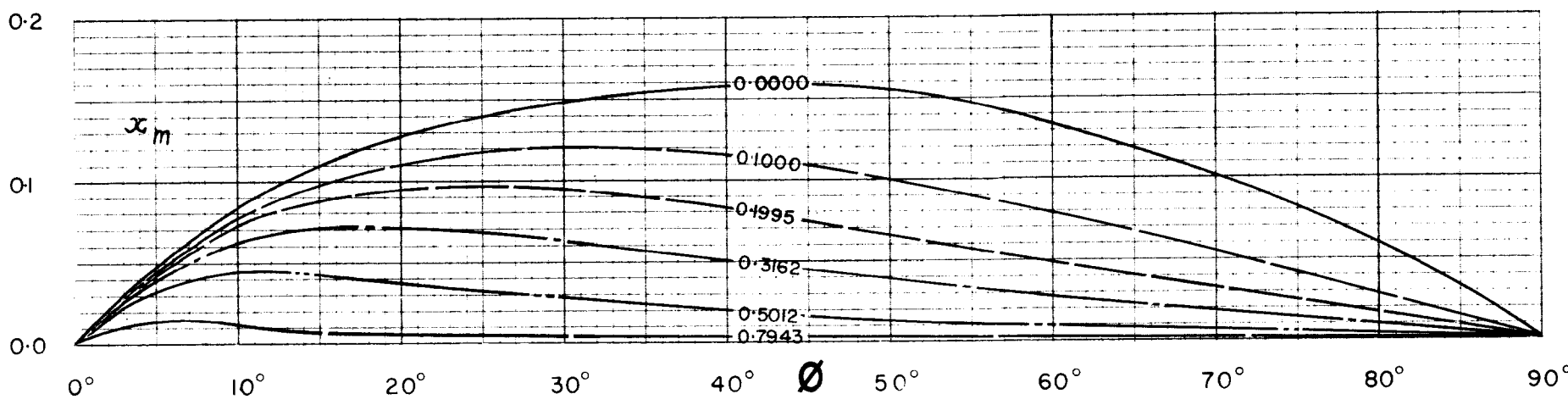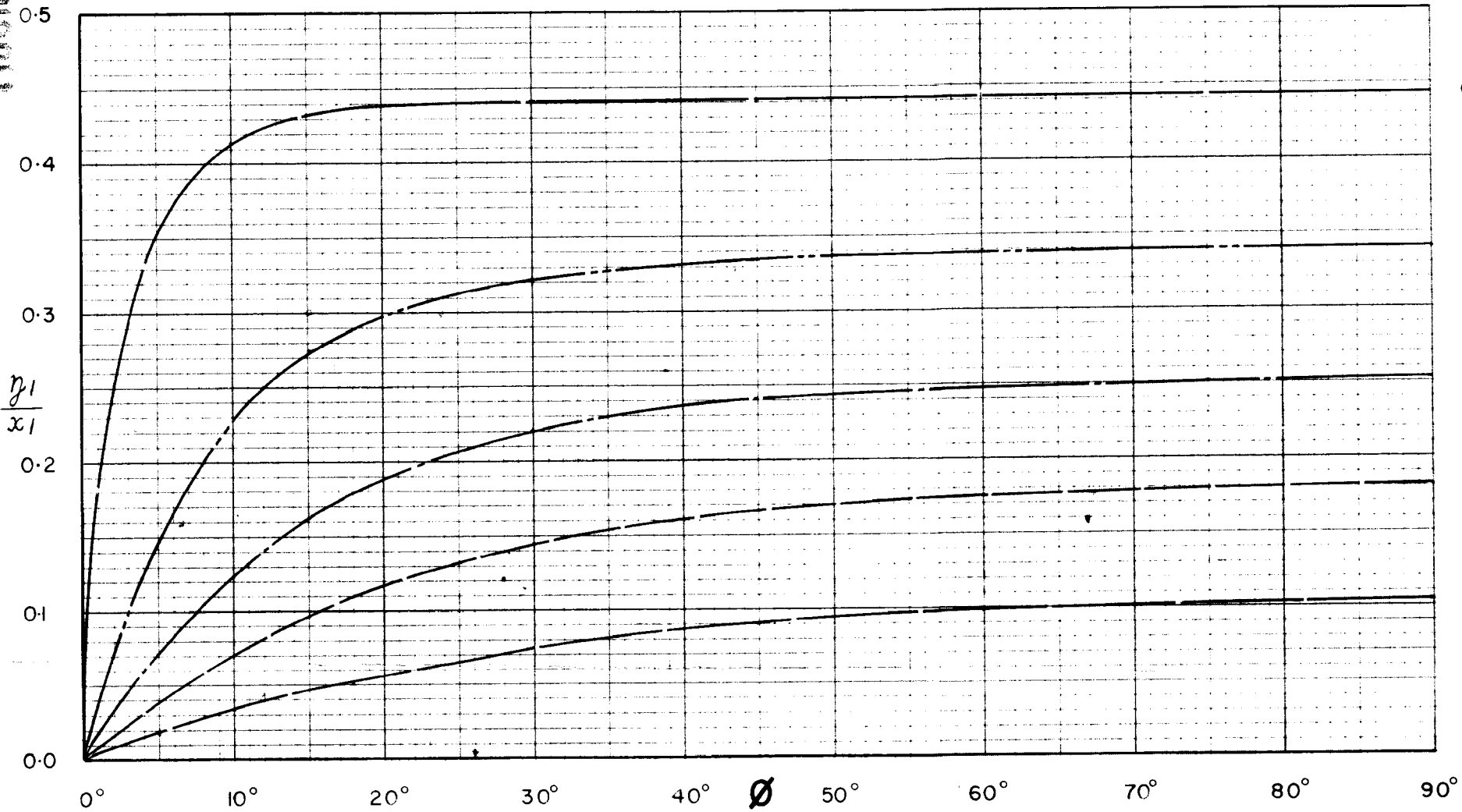

CURVES FOR DETERMINATION OF DIMENSIONS OF SLOPING FEATURE

A

FIG. 25

CURVES FOR DETERMINATION OF DIMENSIONS OF SLOPING FEATURE

B

FIG. 26

$\frac{g_2-g_1}{2\Delta Z}=22$ mgal

$\frac{g_2-g_1}{2}=18$ mgal

$-\log \Delta Z$

$\phi=45°$

$Z_1=0.2$

MILLIGALS

$X_a=1.05$ Km

$X_b=1.7$ Km

log 20·96

"Origin" of mastercurve

"Origin" of (X,G) curve
(i.e. X=1, G=0·1)

KILOMETRES

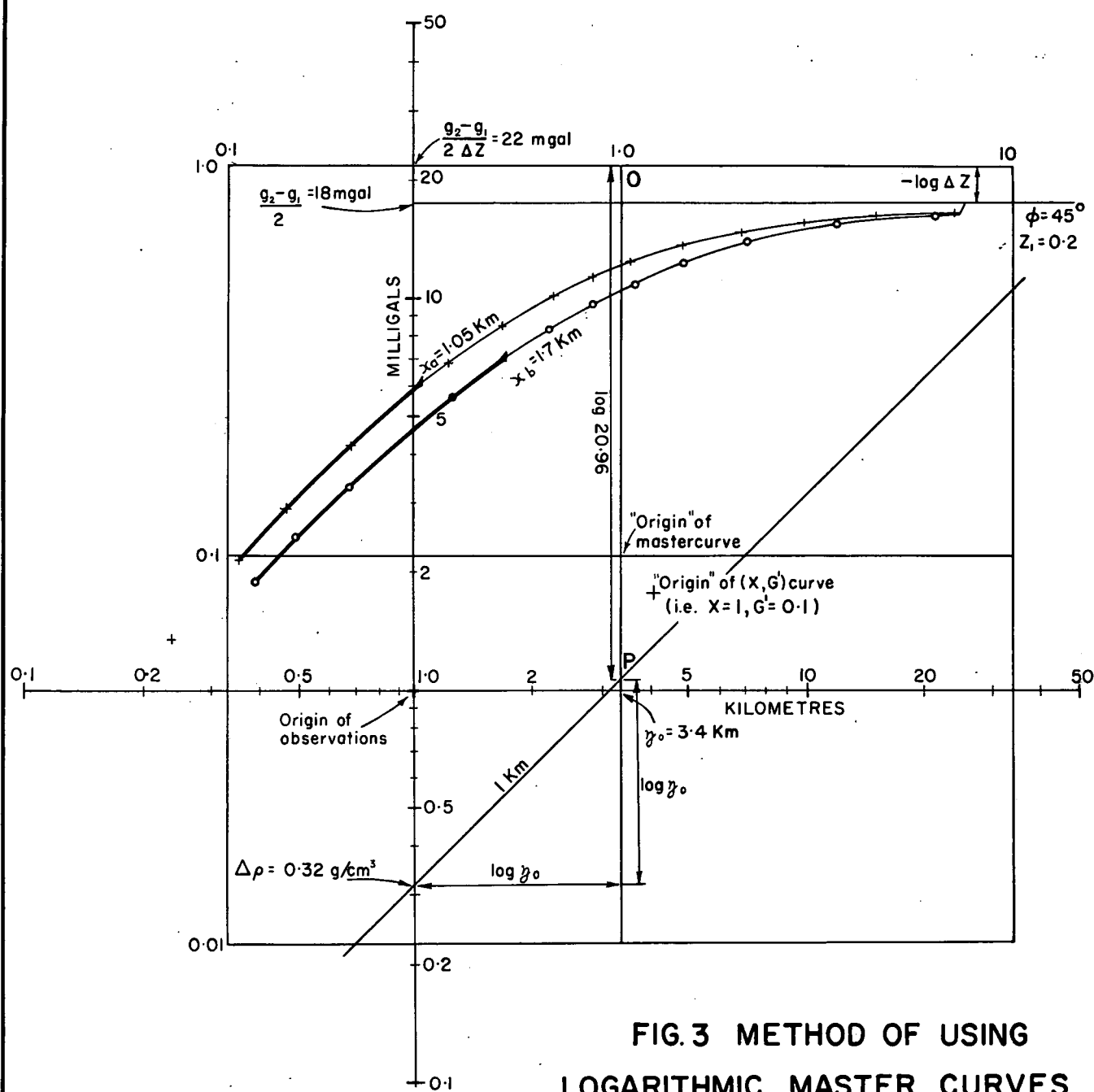Origin of observations

$y_o=3.4$ Km

1 Km

log y_o

log y_o

$\Delta\rho = 0.32$ g/cm³

P

FIG. 3 METHOD OF USING
LOGARITHMIC MASTER CURVES

G 69 — 505

Geophysical Branch, Bureau of Mineral Resources, Geology and Geophysics.
TO ACCOMPANY RECORD No. 1966/86